의학박사 학위논문

유방암 환자 유래 이종이식 모델의 생착과 관련된 요인 연구

Factors associated with engraftment success of patient-derived xenografts of breast cancer

울 산 대 학 교 대 학 원
의 학 과
이 종 원

유방암 환자 유래 이종이식 모델의 생착과 관련된 요인 연구

지 도 교 수　이 희 진

이 논문을 의학박사 학위 논문으로 제출함

2024년 8월

울 산 대 학 교　대 학 원
의 학 과
이 종 원

이종원의 의학박사학위 논문을 인준함

심사위원장 공 경 엽 (인)
심사위원 이 희 진 (인)
심사위원 김 지 선 (인)
심사위원 송 인 혜 (인)
심사위원 정 병 관 (인)

울 산 대 학 교 대 학 원
2024년 8월

Abstract

Background Patient-derived xenograft (PDX) models serve as a valuable tool for the preclinical evaluation of novel therapies. They closely replicate the genetic, phenotypic, and histopathological characteristics of primary breast tumors. Despite their promise, the rate of successful PDX engraftment varies widely in the literature. This study aimed to identify the key factors associated with successful PDX engraftment of primary breast cancer and to provide a comprehensive literature review of factors influencing PDX engraftment success.

Methods We integrated clinicopathological data with morphological attributes quantified using a trained artificial intelligence (AI) model to identify the principal factors affecting PDX engraftment. A comprehensive literature search was conducted using PubMed, Embase, and Web of Science databases to identify studies reporting PDX engraftment success rates and associated factors.

Results Multivariate logistic regression analyses demonstrated that several factors, including a high Ki-67 labeling index (Ki-67LI) ($p<0.001$), younger age at diagnosis ($p=0.032$), post neoadjuvant chemotherapy (NAC) ($p=0.006$), higher histologic grade ($p=0.039$), larger tumor size ($p=0.029$), and AI-assessed higher intratumoral necrosis ($p=0.027$) and intratumoral invasive carcinoma ($p=0.040$) proportions, were significant factors for successful PDX engraftment (area under the curve [AUC] 0.905). In the NAC group, a higher Ki-67LI ($p<0.001$), lower Miller-Payne grade ($p<0.001$), and reduced proportion of intratumoral normal breast glands as assessed by AI ($p=0.06$) collectively provided excellent prediction accuracy for successful PDX engraftment (AUC 0.89).

The literature review revealed that the choice of mouse strain, implantation site and estrogen receptor (ER) status significantly influenced breast PDX engraftment success. Orthotopic implantation yielded higher success rates, including intraductal injection of breast carcinoma cells, and ER-negative tumors with a higher histologic grade showed higher engraftment rates.

Conclusions We found that high Ki-67LI, younger age, post-NAC status, higher histologic grade, larger tumor size, and specific morphological attributes were significant factors for predicting successful PDX engraftment of primary breast cancer. The literature review highlighted the complex interplay of factors influencing breast PDX engraftment success across different factors including implantation site, hormonal status, histologic grade, and underscored the need for careful consideration of these variables in the design and interpretation of PDX studies.

Keywords: Breast cancer, Patient-derived xenograft, Engraftment, Deep learning, Artificial intelligence, Morphometrics, Neoadjuvant chemotherapy, Young age, Triple-negative breast cancer

Contents

List of Figures

List of Tables

Chapter 1. Integrative introduction

This chapter delves into the impact of breast cancer, which remains one of the most diagnosed cancers in women globally and discuss the use of patient-derived xenograft (PDX) models, which are essential for replicating the complex genetic and phenotypic characteristics of original tumors, thus providing a crucial platform for testing new therapies. The success of these models varies, influenced by factors such as tumor grade, subtype, particularly triple-negative breast cancers, and hormonal environment. While innovations like artificial intelligence offer supplementary tools, the primary focus is on the intricacies of PDX model establishment and their pivotal role in developing personalized treatment approaches. This introduction sets the stage for further exploration of how cutting-edge methods can be integrated with traditional approaches to tackle the challenges in breast cancer treatment and improve patient outcomes.

1.1 Background on Breast Cancer

Breast cancer remains a formidable adversary in the realm of public health, consistently ranking as the most common malignancy among women in most parts of the world. Its prevalence and the mortality rates associated with it paint a sobering picture of its impact on society. The disease's epidemiology reveals not only a significant health burden but also highlights disparities in incidence and outcomes across different populations and geographic regions. These disparities are influenced by a range of factors, including genetics, lifestyle, and access to healthcare services, underscoring the complex interplay of socioeconomic, environmental, and biological factors that contribute to breast cancer risk and patient outcomes.

The significance of breast cancer extends beyond its status as a common cancer; it serves as a bellwether for changes in oncological practices and patient care standards. Over the decades, advancements in screening and treatment have improved survival rates, particularly in developed countries where regular mammography screenings and comprehensive treatment options are more accessible. However, in low- and middle-income countries, where such resources are limited, late-stage diagnosis is more common, and the mortality rates remain disproportionately high.

1.1.1 Epidemiology and Significance

Breast cancer is the most commonly diagnosed cancer among women, accounting for 24% of all female cancers and is the leading cause of cancer-related death among women worldwide (1) It represents a significant portion of the global cancer burden, constituting 11.6% of all cancers across both sexes, making it the second most common cancer overall

(2). This disease significantly impacts public health, not only due to its prevalence but also because of its mortality, with an estimated 2.1 million new cases and 627,000 deaths globally in 2018 (1).

Incidence rates of breast cancer have displayed a dynamic pattern over recent decades, particularly in different socioeconomic regions. While most low- and middle-income countries have seen a rise in incidence rates, high-income countries like the USA, Canada, the United Kingdom, France, and Australia experienced a decline in the early 2000s(3). This decline was partly attributable to decreased use of postmenopausal hormone treatment following revelations from the Women's Health Initiative trial, which linked such treatments to an increased risk of developing breast cancer. Despite these fluctuations, the overall global burden of breast cancer continues to grow, primarily due to aging populations.

Geographically, the incidence of invasive breast cancer (IBC) varies significantly, with the highest risk observed in affluent regions such as North America, Europe, and Australia, where up to 9% of women are diagnosed with IBC before the age of 75 (4). This variation is not only a reflection of genetic predispositions but also of lifestyle and environmental factors, as evidenced by studies of migrant populations. These studies show that migrants moving from low- to high-risk areas often see their risk of breast cancer escalate to match that of the host country within one or two generations, suggesting a substantial influence of environmental factors in the etiology of this disease (5).

The heterogeneity of breast cancer is also evident in the prevalence of its various subtypes, which vary significantly by population characteristics and screening practices. In populations where regular screening is common, hormone receptor-positive cancers are most prevalent, with HER2-positive cancers making up 10-15% and ER-negative/HER2-negative cancers accounting for 13-17% of cases. Conversely, in unscreened populations, there is a higher frequency of more aggressive subtypes, with ER-negative/HER2-negative cancers representing 20-40% of cases and HER2-positive cancers comprising 15-25% (6).

The epidemiology of breast cancer thus underscores the urgent need for targeted public health strategies and personalized treatment approaches. Understanding these patterns is crucial for developing interventions that can effectively reduce the incidence and improve the outcomes of breast cancer globally, making epidemiological studies a cornerstone of ongoing research in oncological health.

1.1.2 Challenges in Treatment Due to Tumor Heterogeneity

The genetic landscape of breast cancer is one of the reasons that complicates its treatment. The disease exhibits a notable familial clustering, with high-penetrance genes like BRCA1 and BRCA2 significantly elevating risk, alongside a spectrum of other genes identified through genome-wide association studies that confer moderate to low risks(7).

These genetic factors not only predispose individuals to breast cancer but also influence the subtype and severity of the disease they are likely to develop. Germline mutations in BRCA1 and BRCA2, for instance, are associated with different risks for subtypes such as triple-negative and hormone receptor-positive breast cancers (8).

Pathogenetically, breast cancer can follow multiple pathways, reflecting its molecular heterogeneity. Distinct models of breast cancer initiation and progression have been described, largely based on hormone receptor status. The ER-positive pathway typically progresses from precursors like atypical ductal hyperplasia to invasive and metastatic carcinoma, whereas the ER-negative pathway may begin from lesions like ER-negative ductal carcinoma in situ (DCIS)(9). Each pathway involves distinct genetic alterations and molecular characteristics, such as the frequent TP53 mutations in ER-negative cancers and the different patterns of genetic gains and losses between ER-positive and ER-negative cancers(10).

This intricate web of etiological factors and pathogenic pathways underpins the challenges in treating breast cancer. The variability within and between tumors necessitates a highly personalized approach to treatment, which must consider the individual's genetic background, and the specific molecular characteristics of their tumor.

1.1.3 Importance of Patient-Derived Xenograft (PDX) Models

Given the complexity and variability of many types of cancers, PDX models have become an essential tool in oncology research. These models involve transplanting human tumors into immunocompromised mice, allowing researchers to study the biology of cancer and assess the efficacy of potential treatments in a controlled yet biologically relevant environment. PDX models maintain the histological and genetic integrity of the human tumors from which they are derived, providing a more accurate representation of patient tumors than traditional cell line-based models.

PDX models are particularly valuable for testing drug responses and understanding the mechanisms of resistance that emerge during cancer treatment. By using these models, researchers can observe how different types of breast cancer respond to therapies in real-time, providing insights that are crucial for the development of more effective and personalized treatment strategies. Moreover, these models are instrumental in the preclinical evaluation of new drugs and therapeutic combinations, helping to predict their efficacy before clinical trials in humans.

1.2 Establishing PDX Models

1.2.1 Factors Influencing PDX Model Success

The utility of PDX models in clinical research hinges significantly on their capacity to

faithfully replicate human tumor biology in a controlled experimental context. Several critical factors influence the success of these models, including the origin and handling of the tumor tissue, the immunocompatibility of the host, and the methodological rigor of engraftment procedures. Key among these is the choice of the mouse strain. Studies indicate that immunodeficient mouse strains such as non−obese diabetic /severe combined immunodeficiency (NOD/SCID), NOD scid gamma (NSG), and nude mice significantly affect engraftment outcomes. NSG and NOD/SCID mice, for instance, generally demonstrate higher engraftment rates compared to nude mice, with rates in breast cancer studies ranging from 23% to 77% in NSG and NOD/SCID mice, whereas rates in nude mice have been lower, between 2.5% and 13% (11−17).

Additionally, the implantation site plays a crucial role in the success of PDX engraftment. Orthotopic implantation, which involves placing the tumor tissue into its original anatomical location, often results in higher engraftment rates compared to heterotopic implantation (e.g., subcutaneous) (18-20). This methodological distinction highlights the importance of replicating the natural tumor microenvironment as closely as possible to maximize the biological relevance and translational value of the models.

1.2.2 Engraftment Rates and Challenges in Breast Cancer PDX

Despite their potential, the application of PDX models in breast cancer research is plagued by low engraftment rates and significant variability in tumor take rates. In studies where engraftment rates were explicitly mentioned, the overall take rate varied considerably, with certain types of breast cancer, such as molecular apocrine tumors, showing higher engraftment rates compared to others like Luminal A and B. This variability can also be attributed to the specific method of engraftment employed. For instance, intraductal engraftment has shown higher success rates, up to 77% in one study(16), underscoring its efficacy over more common methods such as subcutaneous engraftment, which typically yields lower take rates (11,12,15,17-19,21).

Furthermore, histological grade has been identified as a factor, with higher-grade tumors typically showing better engraftment rates. This finding suggests that more aggressive tumors may adapt more readily to the xenograft environment, although this can vary depending on other conditions such as whether the tumor samples were chemotherapy-naïve or from patients undergoing neoadjuvant chemotherapy (NAC). Studies have indicated that tumor response to chemotherapy, particularly in TNBC samples from the NAC group, correlates with higher engraftment rates (15,17).

Overall, these insights not only add granularity to the understanding of PDX model variability but also highlight the critical need for meticulous planning and execution of engraftment protocols. By addressing these nuanced factors, researchers can better harness the full potential of PDX models in translational cancer research, ultimately enhancing the

development of personalized therapeutic strategies for breast cancer.

1.3 Role of AI in breast cancer

1.3.1 AI in histopathology and morphometric analysis.

AI has revolutionized the field of histopathology by enabling the extraction and detailed analysis of morphometric features from breast cancer tissue samples. Utilizing advanced algorithms, AI systems can identify and measure nuanced morphological characteristics of tumors, and could reproduce human judgement or excel them at some points (22,23). This capability is critical for understanding the intricate tumor characteristics that dictate disease progression and response to treatment. Recent studies regarding breast cancer also highlight AI's potential in enhancing diagnostic accuracy, notably in the automatic classification of breast cancer subtypes, such as invasive ductal carcinoma (IDC), showcasing the technology's precision and reliability (24,25)

1.4 Study objectives

The overarching goal of this research is to comprehensively analyze and identify the key factors that contribute to the success of PDX engraftment in primary breast cancer. This involves an integrative approach that combines clinicopathological data with advanced AI-driven morphometric analysis.

1.4.1 Identifying key predictors of successful PDX engraftment

The first objective of this study is to determine the principal factors that influence the likelihood of successful PDX engraftment. Utilizing multivariate logistic regression analyses, this research aims to explore how variables such as Ki-67 labeling index, age at diagnosis, and post-neoadjuvant chemotherapy status correlate with engraftment outcomes. The study will particularly focus on the predictive value of these factors, with an emphasis on their quantifiable impact on the engraftment process.

1.4.2 Quantifying morphological attributes affecting PDX success

In tandem with clinical and pathological analyses, this study seeks to employ a trained AI model to quantify specific morphological attributes that may influence the success of PDX engraftments, such as the extent of intratumoral necrosis and the proportion of carcinoma. This objective strives to harness the power of AI to provide a detailed assessment of tumor histology, thereby enhancing the predictive accuracy of PDX model success.

Chapter 2. Factors Associated with Engraftment Success of Patient-Derived Xenografts of Breast Cancer

This work has been accepted in "Lee, J., Lee, G., Park, H.S. et al. Factors associated with engraftment success of patient-derived xenografts of breast cancer. Breast Cancer Res 26, 49 (2024). https://doi.org/10.1186/s13058-024-01794-w."

2.1 Abstract

Background: PDX models serve as a valuable tool for the preclinical evaluation of novel therapies. They closely replicate the genetic, phenotypic, and histopathological characteristics of primary breast tumors. Despite their promise, the rate of successful PDX engraftment is various in the literature. This study aimed to identify the key factors associated with successful PDX engraftment of primary breast cancer.

Methods: We integrated clinicopathological data with morphological attributes quantified using a trained artificial intelligence (AI) model to identify the principal factors affecting PDX engraftment.

Results: Multivariate logistic regression analyses demonstrated that several factors, including a high Ki-67 labeling index (Ki-67LI) ($p<0.001$), younger age at diagnosis ($p=0.032$), post neoadjuvant chemotherapy (NAC) ($p=0.006$), higher histologic grade ($p=0.039$), larger tumor size ($p=0.029$), and AI-assessed higher intratumoral necrosis ($p=0.027$) and intratumoral invasive carcinoma ($p=0.040$) proportions, were significant factors for successful PDX engraftment (area under the curve [AUC]: 0.905). In the NAC group, a higher Ki-67LI ($p<0.001$), lower Miller-Payne grade ($p<0.001$), and reduced proportion of intratumoral normal breast glands as assessed by AI ($p=0.06$) collectively provided excellent prediction accuracy for successful PDX engraftment (AUC: 0.89).

Conclusions: We found that high Ki-67LI, younger age, post-NAC status, higher histologic grade, larger tumor size, and specific morphological attributes were significant factors for predicting successful PDX engraftment of primary breast cancer.

2.2 Introduction

PDX models have emerged as a valuable tool in breast cancer research, allowing for the development of personalized therapies and the study of tumor biology. However, the

success rate of PDX engraftment in breast cancer has been relatively low, hindering the widespread use of this model.

In this study, we analyzed clinicopathologic factors and quantitatively assessed morphometric features extracted by AI to identify features associated with the success of PDX engraftment of primary breast cancer.

2.3 Materials and Methods

2.3.1 Patient population and case selection

Patients enrolled in this study had histologically confirmed invasive breast cancer with tumors larger than 1 cm that were detected through physical examination or imaging. Those who achieved radiologic complete remission or a significant reduction in tumor mass following NAC were excluded. A total of 380 surgically resected tumor samples were collected from 2016 to 2021 at Asan Medical Center. These samples were obtained from patients who consented to undergo breast-conserving surgery, mastectomy, axillary lymph node dissection, or metastasectomy. Eight cases were subsequently excluded due to premature deaths of the engrafted mice, leaving 372 breast cancer cases for the final evaluation. Patients enrolled in this study had histologically confirmed invasive breast cancer with tumors larger than 1 cm that were detected through physical examination or imaging. Those who achieved radiologic complete remission or a significant reduction in tumor mass following neoadjuvant Breast cancer is one of the most diagnosed cancers in women worldwide and it continues to be a significant cause of morbidity and mortality. Despite the numerous advancements in cancer treatment, the heterogeneity and complexity of breast tumors have presented significant obstacles in identifying effective therapies for individual patients. PDX models offer a promising solution to this problem by enabling the testing of novel therapies in preclinical models that more accurately reflect the genetic, phenotypic, and histopathological features of the original tumors. However, establishing PDX models remains a challenging and resource-intensive process. Many factors impact the success of PDX models, including the quality of the tumor sample, the choice of engraftment site, the use of immune-deficient mice, and the timing and method of engraftment (28). In particular, the low engraftment rate of PDX models has been a major obstacle to their widespread use in preclinical studies (29).

Among all types of tumors, breast cancers have been shown to be particularly challenging when it comes to establishing PDX engraftment. Breast cancer has historically exhibited relatively low but diverse engraftment success rates, ranging from 8% to 77% (11,16). Factors associated with successful breast cancer PDX engraftment include applying

hormonal supplementation (e.g., estrogen pellets) and using tumor samples with: a higher histologic tumor grade, from specific tumor subtypes (e.g., triple-negative breast cancer [TNBC]), or from metastatic tumors (11,13,14). Additionally, selecting appropriate host strains for the specific xenograft type can contribute to improved engraftment outcomes (28).

2.3.2 Clinicopathologic data acquisition

Clinicopathological features were gathered from the patients' medical records, including surgical pathology reports. The histopathological findings were retrospectively reviewed for all 372 surgical specimens. The pT and pN categories were evaluated based on the 8th edition of the American Joint Committee on Cancer cancer staging system (30). When NAC was conducted, the residual cancer burden (RCB) and Miller-Payne grade were also assessed.

Estrogen receptor (ER) and progesterone receptor (PR) status were determined through immunohistochemical staining of formalin-fixed, paraffin-embedded tumor tissue sections. Positive staining was defined as nuclear staining in at least 1% of the tumor cells, and the hormone receptor-positive (HR+) type was defined as ER and/or PR IHC-positive.

HER2 status was determined using both immunohistochemistry and, in equivocal cases, silver in situ hybridization according to the guidelines from the American Society of Clinical Oncology/College of American Pathologists (31). HER2 positivity was defined as IHC 2+ or 3+, or a SISH amplification ratio of HER2 gene signals to chromosome 17 signals greater than 2.0.

The percentage of tumor cells showing any degree of nuclear staining for Ki-67LI was recorded for each tumor. These percentages were recorded in increments of 10% as follows: 0 for 0-10%, 10 for 10-20%, 20 for 20-30%, 30 for 30-40%, 40 for 40-50%, 50 for 50-60%, 60 for 60-70%, 70 for 70-80%, 80 for 80-90%, and 90 for 90-100%.

TNBC was defined as a subtype of breast cancer in which the tumor cells did not express ER or PR and also did not exhibit overexpression or amplification of HER2.

Histological TIL levels were estimated for all cases using the methods previously published by a TILs working group (32). TILs were determined by calculating the percentage of the area occupied by mononuclear inflammatory cells within the stromal area of the invasive carcinoma. They were graded with 10% increments as for Ki-67LI.

2.3.3 In vivo tumor implantation and histopathological analysis

All experiments were performed in accordance with the approved protocol and relevant guidelines and regulations. Immediately after resection, the tumor specimens were placed in sterile tissue culture medium (RPM 1640) on ice and immediately transported to the animal

facility at the Asan Institute for Life Sciences, Asan Medical Center, Seoul, Korea. The tumors were orthotopically implanted into the 4th mammary fat pads of female NOD/SCID mice (5 to 8 weeks old) (Koatech Inc., Seoul, Korea). Estrogen pellets were inserted into the subcutaneous soft tissue of the cervical area of the mouse if the grafted tumor was of an HR-positive subtype. Passage cessation was conducted if a mouse showed any abnormal pathological responses, such as jaundice, extreme distress, or the development of lymphoproliferative disease. The tumor size was serially measured, and when the diameter of the implanted tumor reached 1 to 2 cm (~2,000 mm3 in volume), the mice were euthanized. Then, the tumors were excised, cut into ~2 x 2 x 2 mm fragments, and passaged to successive generations of mice.

We used the retrieved PDXs in three distinct ways. The first group was directly implanted into the next passage of mice in a fresh state. The second group was sampled, fixed in formalin, and then embedded in paraffin blocks. These samples were subsequently stained with hematoxylin and eosin. The stained samples were reviewed for histomorphology by two pathologists (J.L. and H.L.), who compared them with the original slides of the surgically removed tumors that had been grafted. The third group was used to preserve the graft. The tissue was placed in vials containing a mixture of dimethyl sulfoxide and fetal bovine serum (1:9) and kept at -70°C for 24 hours. The vials were then placed in liquid nitrogen tanks (-197°C) for long-term storage.

In the initial passage (P1), direct transplantation into female NOD/SCID mice was conducted, typically involving 1-2 mice per patient sample in the first passage (P1), multiplying the number of mice per patient sample as the passage progressed until the last (4th) passage (P4).

2.3.4 PDX engraftment of primary breast cancer: multi-passage

The results of PDX engraftments are shown in Figure 2.1. The first passage (P1) involving grafting 353 distinct primary breast cancer samples into 372 mice. Each mouse received a unique cancer sample, accounting for 336 out of the 353 cancer cases. In the remaining instances, some cancer cases were engrafted into multiple mice. Fifteen cancer cases were each engrafted into two mice, and engraftment success was achieved in five mice from three cases. Moreover, two specific cancer cases were each grafted into three mice; however, successful grafts were not achieved from any of these.

Among the 372 mice included in this passage, we observed 61 instances of successful engraftment, as confirmed by evaluating H&E-stained slides of the engrafted tumors. This indicated an overall success rate of 16.4%, with successful engraftment of 59 out of 353 cases, resulting in a case success rate of 16.7%. During the second passage (P2), we engrafted 57 primary breast cancer samples into a total of 193 mice, with the number of mice per case ranging from 1 to 15. Of the 193 mice involved, 158 demonstrated successful

engraftment, resulting in an overall success rate of 81.9%. Successful engraftment occurred in 52 out of the 57 cases, resulting in a case success rate of 91.2%.

The third passage (P3) involved grafting 33 distinct primary breast cancer cases into 304 mice. This passage displayed a consistently high success rate, with successful engraftment observed for 239 out of 304 mice, representing an overall success rate of 78.6%. We observed successful engraftment of 29 out of 33 cases, resulting in a case success rate of 87.9%.

In the fourth passage (P4), we conducted larger-scale experiments involving four distinct primary breast cancer cases and a total of 102 mice. We observed successful engraftment of 69 out of 102 mice, resulting in an overall success rate of 67.6%. All four cases of breast cancer in P4 resulted in successful engraftment, maintaining a case success rate of 100%.

2.3.5 Engraftment success across sequential PDX passages and associated clinicopathological factors: metastasectomy cases (n=19)

In the context of tissue samples from metastatectomies, the first PDX passage included 19 cases, with the majority being single-mouse grafts (16 out of 19), and included a total of 22 mice. This passage yielded an overall engraftment success rate of 18.2% (4/22 mice) and a case-based success rate of 21.1% (4/19 cases). No statistically significant difference in PDX engraftment rate was observed between breast mastectomy and metastatectomy samples (p=0.859).

The second passage involved 4 metastatectomy cases and 13 mice, achieving an overall success rate of 53.8% (7/13 mice) and a case success rate of 75% (3/4 cases).

The third passage included 3 metastasectomy cases engrafted into a total of 14 mice. This passage resulted in a 100% overall success rate (14/14 mice) and a 100% case-based success rate (3/3 cases). Finally, the fourth passage involved a single metastasectomy case and 7 mice, maintaining a 100% success rate both overall (7/7 mice) and at the case level (1/1), underlining consistent performance in this phase.

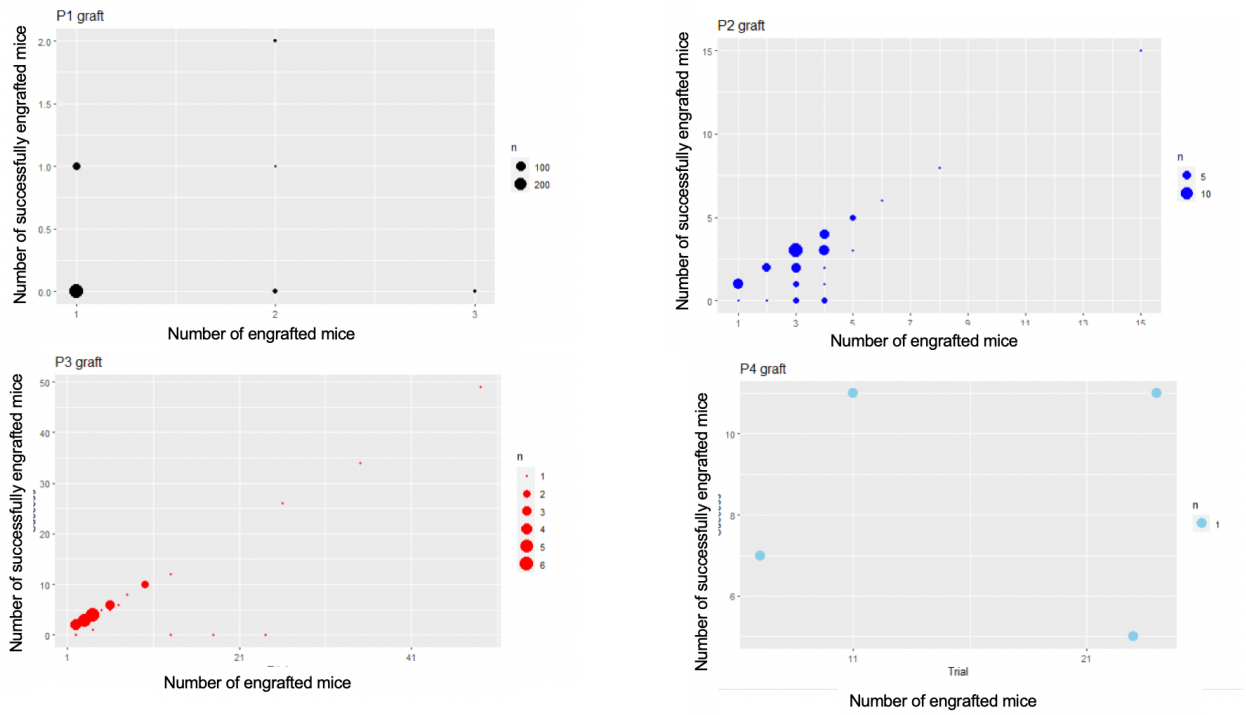

Figure 2.1 Sequential grafting and engraftment success rates of PDXs

Upper left: P1, involving 394 mice from 372 patients, with successful engraftment observed in 65 mice from 63 patient samples; Upper right: P2, involving further transfer of 61 tumors from P1 into an additional 206 mice, resulting in successful engraftment in 165 mice; Lower left: P3, involving engraftment of tumors from 36 patients into 318 mice, with successful engraftment confirmed in 253 mice; Lower right: P4, involving transfer of tumors from 4 patients into 109 mice, resulting in successful engraftment in 76 mice.

2.3.6 AI-assisted morphometric analysis

We developed an AI model for morphometric analysis to extract features for the prediction of PDX engraftment. The model was trained on WSIs of H&E stained surgically resected tissues from 64 breast cancer patients, scanned at 400x magnification. The dataset was randomly partitioned into a training set (65%) and a testing set (35%). The ResNet50 architecture, pre-trained on the ImageNet dataset, was implemented. Image augmentation techniques such as color normalization, random rotation, and color jittering were applied solely to the training set. The model was trained using a batch size of 256 with a learning rate of 0.0003 and involved fifteen epochs using the Adam optimization algorithm. Fifteen epochs were performed using the Adam optimization algorithm.

The model processed WSIs into 112 × 112 pixel non-overlapping patches based on morphological similarity. These patches were classified by a consensus meeting between two board-certified pathologists (J.L. and H.L.) into various tissue types, including adipose tissue (Figure 2.2A), background (Figure 2.2B), and necrosis (Figure 2.2C). Furthermore, we employed a unified classification, categorizing both carcinoma in situ and invasive carcinoma under the umbrella patch label 'carcinoma' (Figures 2.2D to G). In terms of

other normal structures of the breast parenchyma, patches of stroma (Figure 2.2H) and terminal ductal lobular units (TDLUs) (Figure 2.2I) were also labeled.

To evaluate TILs, specialized segmentation training was applied to 15 representative breast cancer WSIs. A representative H&E slide was scanned (Figure 2.2J, left side), de-stained, and re-stained with a cocktail of immune cell markers (Figure 2.2J, middle): CD3 (1:50, Novocastra Laboratories, Leica Biosystems, Nussloch, Germany), CD20 (1:500, Novocastra Laboratories), and CD79 (1:200, Dako, Agilent Technologies, Santa Clara, CA, USA), using a Ventana ES automated immunohistochemistry (IHC) stainer according to the manufacturer's protocols (Ventana ES automated IHC stainer, Tucson, AZ, USA). Nuclear immunolabeling in black denoted lymphocytes, and they were spatially matched with the H&Es for TIL annotation. These slides were utilized for training of the segmentation model (Figure 2.2J, right side). which utilized the ResNet-based DeeplabV3+. The model was trained for 50 epochs with a learning rate of 0.001 and a batch size of 16. The segmentation model utilized a combination of the ResNet50 architecture for feature extraction and the DeepLabV3 Plus architecture for semantic segmentation. The learning rate was set to 0.001, the batch size was 16, and the model was trained for 50 epochs.

Upon completing the training phase, our AI model was applied to WSIs obtained from 329 out of the 353 surgically resected primary breast cancers that were used for PDX engraftment. The slides were spatially reconstructed for patch interpretation results and color-coded accordingly (Figure 2.2K and L). They were then compared to the original H&E stained tumor slides by two pathologists (H.L. and J.L.) for evaluation of the AI-predicted features. The AI model exhibited an F1 score of 0.846 when compared to human pathologists; however, nine slides were excluded from the final analysis because the model had difficulty accurately interpreting carcinoma components; specifically, low histologic grade and sparse cellularity carcinomas were mistakenly identified as TDLU (Figure 2.3A, B) or as stroma (Figure 2.3C).

Finally, 320 slides were selected as candidates for further statistical evaluation. The AI model identified patches within the boundaries of the largest tumor, delineating its edges (Figure 2.2M). The proportions of these patches relative to the total number of patches within the tumor perimeter were calculated for the different tissue types, including adipose tissue (adipose tissue intratumoral proportion, AP), necrotic tissue (necrotic tissue intratumoral proportion, NP), terminal ductal lobular units (TDLU intratumoral proportion, TDLUP), stromal tissue (intratumoral proportion of stromal tissue, SP), and invasive carcinoma (invasive carcinoma intratumoral proportion, ICP). ICP was determined by taking the initial estimate of the intratumoral proportions of patches labeled as carcinoma and multiplying by a true invasive carcinoma fraction, which pathologists assessed after a consensus meeting and reviewing all 320 H&E slides.

Tumor-infiltrating lymphocytes intratumoral proportion (TILP) was separately calculated

using the aforementioned segmentation model applied within the tumor boundary to determine the area of TILs. The areas identified as lymphocytes were divided by the total area of intratumoral patches. To facilitate statistical analysis and interpretation, these proportions were multiplied by a factor of 10,000 due to the large denominators involved.

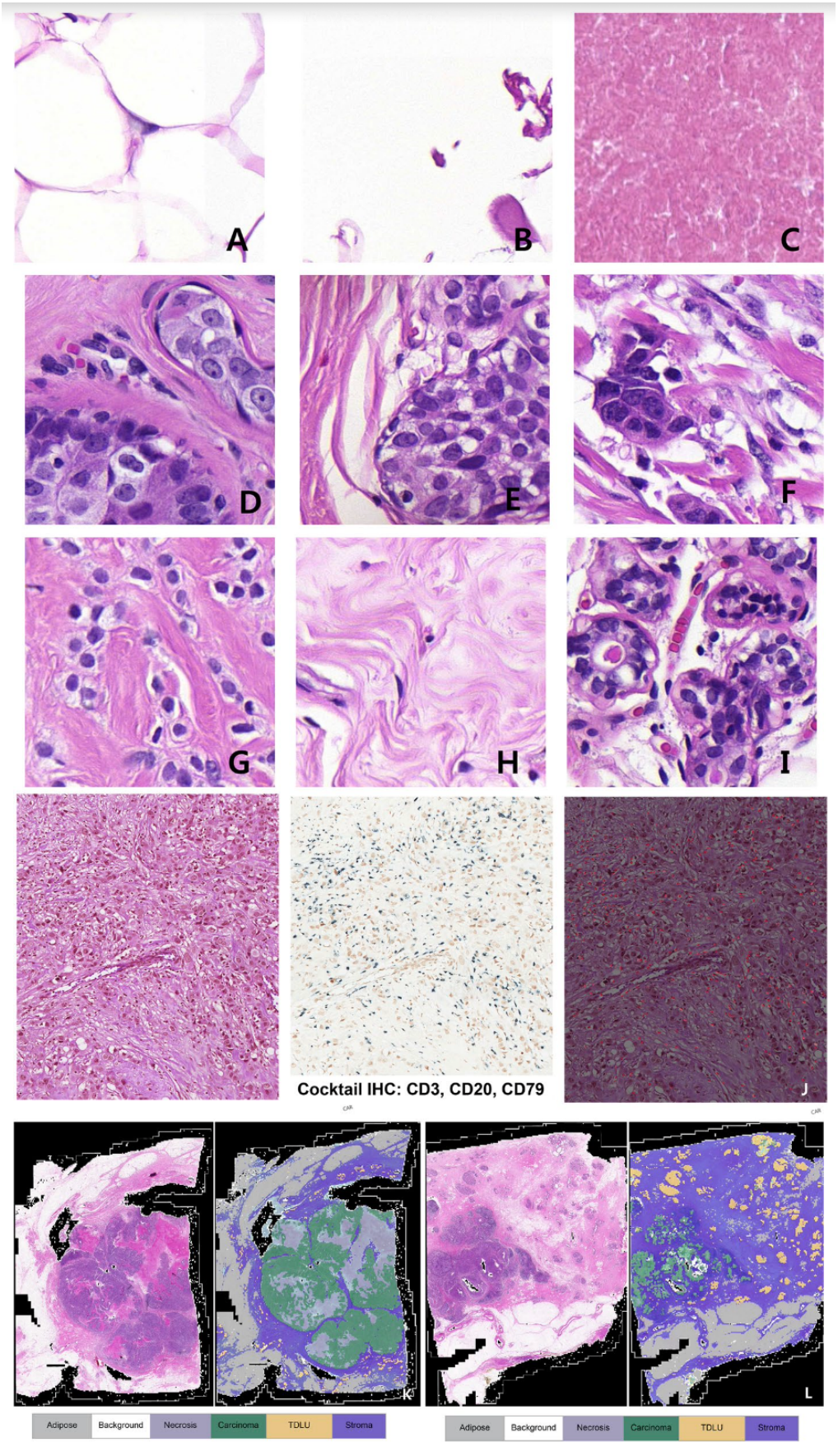

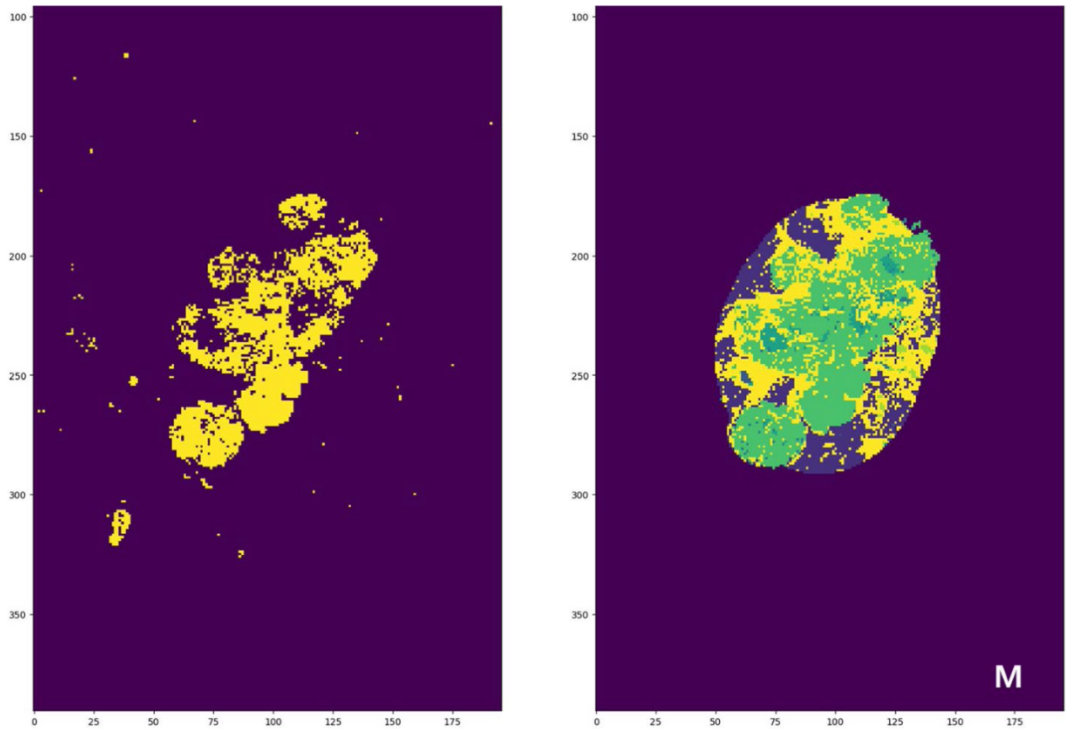

2.2 Artificial intelligence-assesed classification of patches

A. Adipose; B. Background; C. Necrosis; D. Ductal carcinoma in situ, classified as carcinoma; E. Lobular carcinoma in situ, classified as carcinoma; F. Invasive ductal carcinoma, classified as carcinoma; G. Invasive lobular carcinoma, classified as carcinoma; H. Stroma; I. Terminal ductal lobular unit; J. Tumor-infiltrating lymphocytes trained with a segmentation model. Left, hematoxylin and eosin (H&E) stained slide, X100, original magnification. Middle, Cocktail immunohistochemistry (IHC) for identification of lymphocytes, X100, CD3, CD20, and CD79 cocktail IHC, original magnification. Right, red annotation indicating the area of cocktail IHC-stained lymphocytes in the H&E slides (annotated digitally processed image, original magnification, X100). K-L. Representative H&E from successful (K) and failed (L) PDX graft cases and their corresponding AI-model applied images. K. Abundant intratumoral necrosis and carcinoma proportions in the H&E are also highlighted in sky-blue and green in the AI-model applied image, respectively (right); L. Abundant intratumoral TILs, stroma, and TDLU identified in the H&E slide (left) are also highlighted in the AI-categorized image (right). M. algorithm applied to the carcinoma (left side) generated a tumor boundary (right side, yellow) encircling the carcinoma component (right side, green).

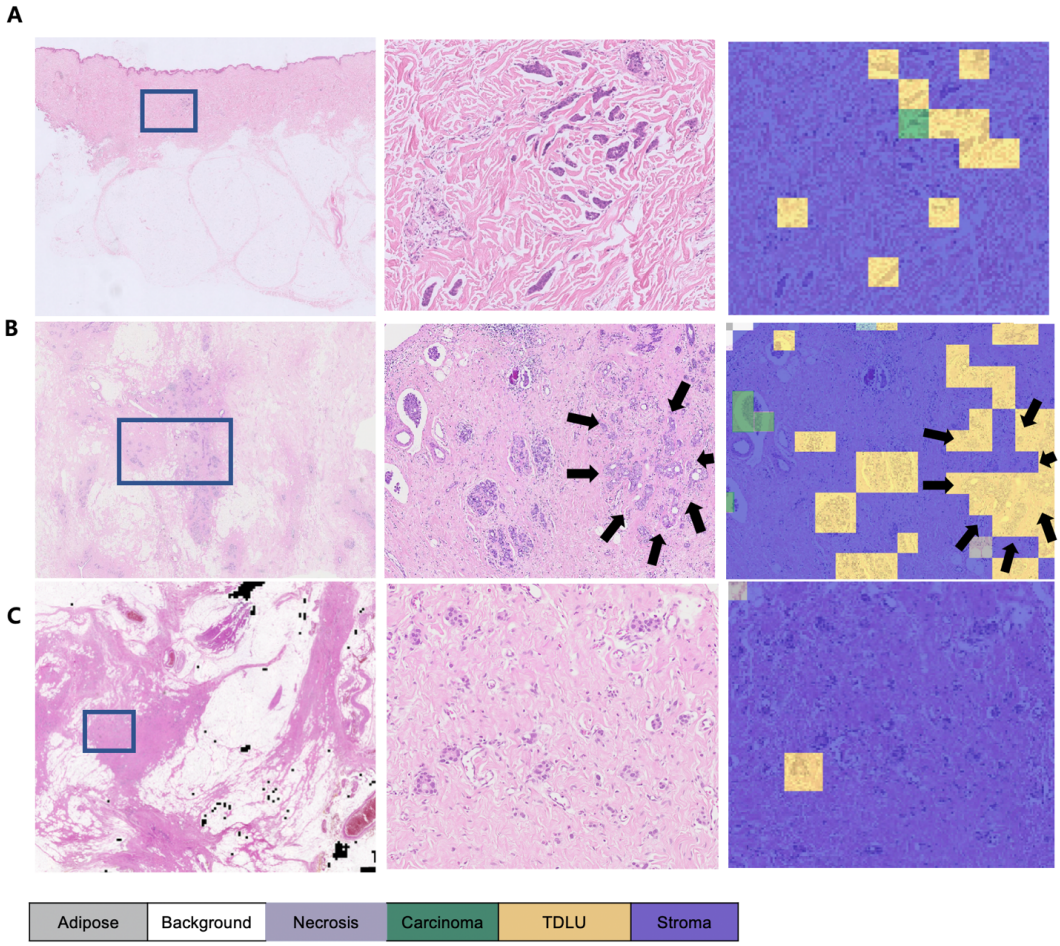

2.3 Failures of identification by the artificial intelligence model

A. Histologic grade 2 invasive carcinoma with low cellularity (left and middle side) is mostly assessed as TDLU (right side, yellow). B. Residual IDC (middle, arrows) with LVI is mostly interpreted as TDLU (right side, yellow) or stroma (right side, purple). C. Low histologic grade IDC with sparse cellularity (middle) is interpreted mostly as stroma (right side, purple).

2.3.7 Statistical analysis

Statistical analyses were performed to assess the clinicopathological data regarding the success of PDX engraftment. Independent sample t-tests and Chi-square tests were used to conduct an exploratory analysis of the data. Following this analysis, logistic regression analyses were used to evaluate the clinicopathologic factors that were associated with PDX engraftment. Initially, all potential predictors were included in the univariate logistic regression analyses. A multivariate logistic regression model was subsequently constructed using a backward stepwise elimination process with the goal of optimizing the Akaike Information Criterion (AIC). All variables with a p-value less than 0.2 in the univariate analysis were considered for inclusion in the multivariate model. The final multivariate model retained only the variables that contributed to a lower AIC value, ensuring a more parsimonious yet explanatory model. To assess the discriminative ability of the logistic

regression models for predicting PDX engraftment, we computed ROC curves and their corresponding area under the curve (AUC) for each model.

Also, recursive partitioning and regression tree classification, as described by Mantzaris et al., were established using the R software package "RPART" (33). To simplify the model and prevent overfitting, a pruning process was conducted on the initial decision tree. The complexity parameter (CP) was selected based on the printcp output, which evaluated the cross-validated error for different CP values. For our tree analyses, a CP value of 0.03 was chosen for pruning, balancing the model complexity, and the predictive accuracy. In the decision tree models, the variable importance was quantified based on the degree of information gain or impurity reduction each variable contributed to the splits at various nodes, which did not necessarily correspond to the most important variables at each node as displayed in the plotted decision trees.

To evaluate the reliability and stability of the logistic regression models and the RPART tree, bootstrap analyses were conducted. A total of 1,000 bootstrap replicates were generated. This resampling procedure was used to estimate the distribution of the AUC. Bias-corrected accelerated (BCa) bootstrap methods were employed to calculate confidence intervals for the AUC. All statistical analyses were conducted using R software version 4.2.1.

2.4 Results

2.4.1 Factors affecting the engraftment success rates of primary breast cancer

The clinicopathological characteristics of the primary breast cancer patient population in relation to the PDX engraftment are summarized in Table 1, and the detailed PDX engraftment success rates across multi-passages are described in Figure 2.1. In the cohort of 353 primary breast cancer patients, the mean age in the engraftment success group was 45.8±11.0 years, significantly younger than the 50.9±12.2 years observed in the engraftment failure group ($p=0.003$). A higher prevalence of TNBC was observed in the success group, accounting for 88.1% (52/59) compared to 32.3% (95/294) in the failure group ($p<0.001$). Ki-67LI was significantly elevated in the success group, with a mean value of 73.2±14.9, compared to 39.0±29.1 in the failure group ($p<0.001$). In terms of NAC treatment, 79.7% (47/59) of the success group was from the NAC group, which was significantly higher than the 37.1% (109/294) in the failure group ($p<0.001$). Tumor size was also significantly different, with the success group averaging 4.1±2.6 cm and the failure group averaging 3.3±2.2 cm ($p=0.019$). The histologic grade was also notably associated with PDX engraftment success, with 91.5% (54/59) of successful cases being histologic grade 3

compared to 48.0% (141/294) in the failure group (p<0.001). Other variables, including diagnosis, LVI, number of positive LNs, TIL%, and AJCC stages showed no significant differences between the success and failure groups.

AI-assessed morphometric features in the cohort of 320 primary breast cancer patients were also analyzed, and significant differences were observed between the failure (n=270) and success groups (n=50) (Table 2). The success group exhibited a significantly lower average AP (p=0.006). Conversely, the success group had a significantly higher NP compared to the failure group (p<0.001), along with a significantly lower TDLUP (p<0.001). Similarly, the success group had a lower SP than the failure group (p=0.007). Although the ICP was higher in the success group (p=0.096), statistical significance was not reached. There were no significant differences in TILP between the groups. Both univariate and multivariate logistic regression analyses were conducted, incorporating a range of clinicopathological variables as well as AI-analyzed morphometric features (Table 3). In univariate analysis, several clinicopathologic factors were found to be significantly related to successful PDX engraftment, including younger age (OR=0.96, CI=0.94-0.99, p=0.005), higher Ki-67LI (OR=1.06, CI=1.04-1.08, p<0.001), TNBC subtype (OR=9.78, CI=1.27-75.23, p=0.028), histologic grade 3 (OR=16.62, CI=5.05-54.71, p<0.001), larger invasive tumor size (OR=1.23, CI=1.09-1.38, p<0.001) and more positive metastatic LNs (OR=1.04, CI=1.00-1.08, p=0.031).

In terms of morphological attributes, a 0.1% increase in NP increased the odds of PDX engraftment by 58% (NP: OR=1.58, CI=1.39-1.80, p<0.001). Conversely, 0.1% increase in AP was associated with a 39% decrease in the odds of PDX engraftment (OR=0.61, CI=0.47-0.79, p=0.035). 0.1% increase in TDLUP resulted in an 82% decrease in PDX engraftment odds (OR=0.18, CI=0.08-0.41, p=0.006), and a 0.1% increase in SP led to a 37% reduction in engraftment odds (OR=0.63, CI=0.46-0.86, p=0.007).

In multivariate logistic regression analysis for the primary breast cancer patients, including chemo-naïve and NAC group, the variables age, Ki-67LI, NAC status, tumor size, histologic grade, NP, ICP, and SP were selected using the stepwise elimination method for the optimal AIC. In the clinicopathologic analysis, significant factors for PDX engraftment included younger age (OR=0.96, CI=0.92-1.00, p=0.032), higher Ki-67LI (OR=1.05, CI=1.02-1.07, p<0.001), NAC status (OR=3.27, CI=1.41-7.60, p=.006), larger tumor size (OR=1.20, CI=1.02-1.41, p=.029), and histologic grade 3 (OR=4.34, CI=1.08-17.53, p=.039). In the analysis of morphometric features, a 0.1% increase in NP increased the odds of success by 92.7% (OR=1.927, CI: 1.077-3.449, p=0.027), and a 0.1% increase in ICP increased the odds of success by 82.0% (OR=1.820, CI: 1.028-3.223, p=0.040). A bootstrap analysis was conducted to validate the multivariate logistic regression analysis predictive model with the generation of 1,000 replicates to assess its reliability. The initial AUC was 0.905, with a bias of 0.0079 and a standard error of 0.0184. The 95% BCa confidence interval for the

AUC ranged from 0.8337 to 0.9296. The optimal cutoff point, determined by Youden's J statistic, was 0.129. At this cutoff, the PPV was 0.40 and the NPV was 0.99 (Figure 2.4A).

We also generated a decision tree model using the RPART algorithm by incorporating both AI-analyzed morphometric and clinicopathological variables for the primary breast cancer group. The model was pruned at various CPs, and the optimal CP was selected based on the minimized cross-validation error.

In terms of variable importance, cancer subtype was the most significant at 20%, followed by tumor size at 14%, NP at 13%, Ki-67LI at 12%, and patient age at 7%. Additional variables such as SP, metastatic LNs, and histologic grade each contributed 6% to the model. (Table 4 and Figure 2.5A).

After bootstrapping with 1,000 replicates, the pruned decision tree model yielded an AUC of 0.8304, accompanied by a bias of 0.0694 and a standard error of 0.041. The 95% confidence interval for the AUC, calculated using the BCa method, ranged from 0.6815 to 0.8511. At the optimal cutoff point determined by Youden's J statistic, which was 0.125, the model yielded a PPV of 0.398 and an NPV of 0.985 (Figure 2.4B).

Table 1 Characteristics of the primary breast cancer patient population based on the success of PDX engraftment

Variable	All (n = 353)			NAC group (n = 156)		
	Failure (n = 294)	Success (n = 59)	*p*-value*	Failure (n = 109)	Success (n = 47)	*p*-value*
Age	50.9 ± 12.2	45.8 ± 11.0	**0.003**	50.4 ± 10.7	45.2 ± 11.0	**0.007**
Subtype			**< 0.001**			**< 0.001**
HER2 +	20 (6.8%)	1 (1.7%)		8 (7.3%)	1 (2.1%)	
HR +	147 (50.0%)	5 (8.5%)		48 (44.0%)	4 (8.5%)	
HR + /HER2 +	32 (10.9%)	1 (1.7%)		16 (14.7%)	1 (2.1%)	
TNBC	95 (32.3%)	52 (88.1%)		37 (33.9%)	41 (87.2%)	
Ki-67LI (%)	39.0 ± 29.1	73.2 ± 14.9	**< 0.001**	33.9 ± 32.3	74.0 ± 15.1	**< 0.001**
NAC			**< 0.001**			
Yes	109 (37.1%)	47 (79.7%)		–	–	
No	185 (62.9%)	12 (20.3%)		–	–	
Diagnosis			0.474			0.176
IDC	262 (89.1%)	53 (89.8%)		198(94.7%)	43(91.5%)	
ILC	7 (2.4%)	0 (0.0%)		2(0.96%)	0(0.0%)	
Adenoid cystic carcinoma	1 (0.3%)	1 (1.7%)		0(0.0%)	0(0.0%)	
Invasive apocrine carcinoma	1 (0.3%)	0 (0.0%)		0(0.0%)	0(0.0%)	
Micropapillary carcinoma	8 (2.7%)	2 (3.4%)		5(2.4%)	2(4.3%)	
Metaplastic carcinoma	8 (2.7%)	3 (5.1%)		1(0.5%)	2(4.3%)	
Mucinous carcinoma	7 (2.4%)	0 (0.0%)		3(1.4%)	0(0.0%)	
Size (cm)	3.3 ± 2.2	4.1 ± 2.6	**0.019**	4.3 ± 2.7	4.6 ± 2.7	0.542
LVI			0.376			0.280
Not identified	163 (55.4%)	37 (62.7%)		53 (48.6%)	28 (59.6%)	
Present	131 (44.6%)	22 (37.3%)		56 (51.4%)	19 (40.4%)	
Number of positive LNs	2.7 ± 8.5	3.2 ± 7.3	0.646	5.6 ± 13.1	4.0 ± 8.0	0.336
TIL (%)	11.0 ± 17.9	9.3 ± 13.6	0.43	4.8 ± 10.3	6.6 ± 9.6	0.303
HG			**< 0.001**			**< 0.001**
2	153 (52.0%)	5 (8.5%)		55 (50.5%)	4 (8.5%)	
3	141 (48.0%)	54 (91.5%)		54 (49.5%)	43 (91.5%)	
pT			0.099			0.433
1	74 (25.2%)	10 (16.9%)		16 (14.7%)	5 (10.6%)	
2	170 (57.8%)	36 (61.0%)		57 (52.3%)	29 (61.7%)	
3	47 (16.0%)	10 (16.9%)		33 (30.3%)	10 (21.3%)	
4	3 (1.0%)	3 (5.1%)		3 (2.8%)	3 (6.4%)	
pN			0.396			0.093
0	154 (52.4%)	35 (59.3%)		34 (31.2%)	25 (53.2%)	
1	85 (28.9%)	12 (20.3%)		35 (32.1%)	10 (21.3%)	
2	32 (10.9%)	5 (8.5%)		23 (21.1%)	5 (10.6%)	
3	23 (7.8%)	7 (11.9%)		17 (15.6%)	7 (14.9%)	
M			1.000			1.000
0	291 (99.0%)	58 (98.3%)		106 (97.2%)	46 (97.9%)	
1	3 (1.0%)	1 (1.7%)		3 (2.8%)	1 (2.1%)	
AJCC stage			0.55			0.213
I	55 (18.7%)	7 (11.9%)		12 (11.0%)	4 (8.5%)	
II	162 (55.1%)	35 (59.3%)		43 (39.4%)	27 (57.4%)	
III	75 (25.5%)	16 (27.1%)		51 (46.8%)	15 (31.9%)	
IV	2 (0.7%)	1 (1.7%)		3 (2.8%)	1 (2.1%)	
Miller Payne grade						**< 0.001**
1	-	-		19 (17.4%)	26 (55.3%)	
2	-	-		39 (35.8%)	10 (21.3%)	

Table 1 (continued)

Variable	All (n = 353)			NAC group (n = 156)		
	Failure (n = 294)	Success (n = 59)	*p*-value*	Failure (n = 109)	Success (n = 47)	*p*-value*
3	-	-		46 (42.2%)	11 (23.4%)	
4	-	-		5 (4.6%)	0 (0.0%)	
RCB score	-	-		3.1 ± 1.0	3.2 ± 1.2	0.659
RCB class						0.052
I	-	-		4 (3.7%)	0 (0.0%)	
II	-	-		44 (40.4%)	28 (59.6%)	
III	-	-		61 (56.0%)	19 (40.4%)	

PDX Patient-derived xenograft, *NAC* Neoadjuvant chemotherapy, *HER2* HER2 positive breast cancer, *HR* + , hormone receptor-positive breast cancer, *TNBC* Triple-negative breast cancer, *Ki-67LI* Ki-67 labeling index, *IDC* Invasive ductal carcinoma, *ILC* Invavsive lobular carcinoma, *LVI* Lymphovascular invasion, *LN* Lymph node, *TIL* Tumor-infiltrating lymphocytes, *HG* Histologic grade, *pT* Pathological tumor stage, *pN* Pathological nodal stage, *M* Metastasis stage, *AJCC* American Joint Committee on Cancer, *RCB* Residual cancer burden

* Bold: significant at *p*-value < 0.05

Table 2 AI-analyzed intratumoral image patch proportions and PDX engraftment success in primary breast cancers

Variable *	All (n = 353)			NAC group (n = 131)		
	Failure (n = 294)	Success (n = 59)	*p*-value**	Failure (n = 93)	Success (n = 38)	*p*-value**
AP	639.9 ± 727.1	409.0 ± 484.0	**0.006**	517.3 ± 622.2	450.9 ± 528.0	0.564
NP	740.7 ± 981.9	1575.0 ± 1264.1	**< 0.001**	901.3 ± 1101.4	1642.8 ± 1358.9	**0.001**
TDLUP	504.4 ± 692.5	219.8 ± 233.3	**< 0.001**	475.2 ± 730.2	201.6 ± 213.9	**0.001**
SP	3377.5 ± 1265.9	2855.3 ± 1094.8	**0.007**	3512.4 ± 1523.4	2855.7 ± 1180.3	**0.019**
TILP	17.8 ± 22.8	15.0 ± 15.9	0.285	10.2 ± 14.0	11.3 ± 13.3	0.678
ICP	4208.0 ± 1450.8	4571.6 ± 1201.5	0.096	3056.0 ± 1470.1	3271.5 ± 1174.1	0.423

AP Adipose proportion, *NP* Necrosis proportion, *BP* Background proportion, *TDLUP* Terminal ductal lobular unit proportion, *SP* Stroma proportion, *TILP* Tumor-infiltrating lymphocyte proportion, *ICP* Invasive carcinoma proportion;

* Values scaled up by 10,000

** Bold: significant at *p*-value < 0.05

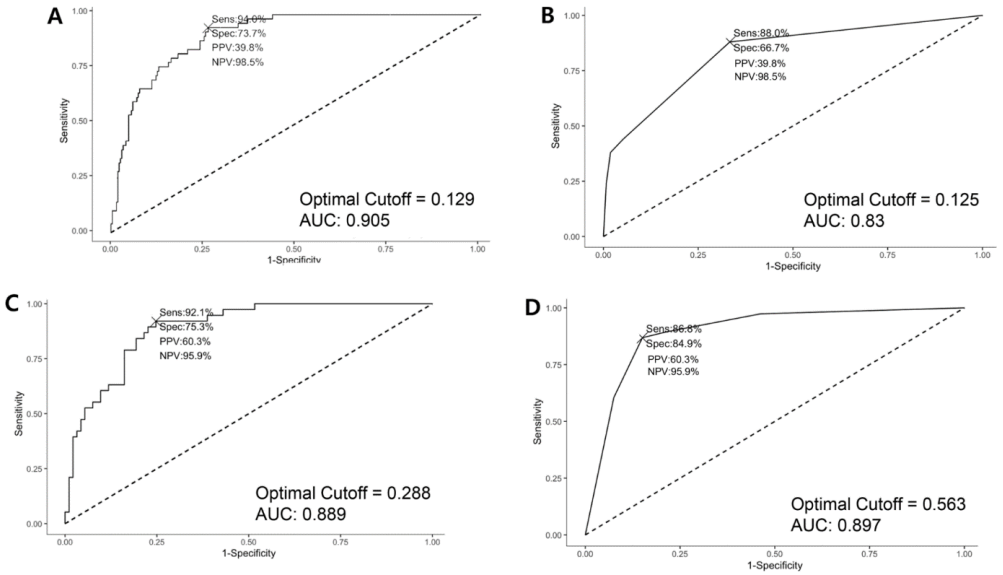

Figure 2.4. Receiver-operated curves for predictive models of engraftment success

A. Multivariate logistic regression of primary breast cancers, including both chemo-naïve and neoadjuvant chemotherapy (NAC) treated groups, incorporating the selected variables from both AI-evaluated morphometric features and clinicopathological findings. B. Pruned decision tree prediction model using clinicopathological and AI-derived morphometric features for primary breast cancers including both chemo-naïve and NAC treated groups. C. Multivariate logistic regression model for the NAC group. incorporating the selected variables from both AI-evaluated morphometric features and clinicopathological findings. D. Pruned decision tree prediction model in the NAC group, utilizing both clinicopathological and AI-derived morphometric features.

Table 3 Logistic regression analyses of clinicopathologic factors and AI-analyzed image data impacting PDX engraftment

Variable*		All (n = 320) Failure (n = 270)	Success (n = 50)	Univariate ** (Odds ratio, 95% CI, *p*-value***)	Multivariate ** (Odds ratio, 95% CI, *p*-value***)	Variable*		NAC group (n = 131) Failure (n = 93)	Success (n = 38)	Univariate ** (Odds ratio, 95% CI, *p*-value***)	Multivariate** (Odds ratio, 95% CI, *p*-value***)
AP	Mean ± SD	639.9 ± 727.1	409.0 ± 484.0	**0.61 (0.47–0.79, *p* = 0.035)**		AP	Mean ± SD	517.3 ± 622.2	450.9 ± 528.0	0.82 (0.74–0.91, *p* = 0.562)	
NP	Mean ± SD	740.7 ± 981.9	1575.0 ± 1264.1	**1.58 (1.39–1.80, *p* < 0.001)**	**1.927 (1.077–3.449, *p* = 0.027)**	NP	Mean ± SD	901.3 ± 1101.4	1642.8 ± 1358.9	**1.60 (1.38–1.85, *p* = 0.003)**	
TDLUP	Mean ± SD	504.4 ± 692.5	219.8 ± 233.3	**0.18 (0.08–0.41, *p* = 0.006)**		TDLUP	Mean ± SD	475.2 ± 730.2	201.6 ± 213.9	**0.22 (0.18–0.27, *p* = 0.034)**	0.181 (0.033–1.00, *p* = 0.06)
SP	Mean ± SD	3377.5 ± 1265.9	2855.3 ± 1094.8	**0.63 (0.46–0.86, *p* = 0.007)**	1.545 (0.844–2.827, *p* = 0.159)	SP	Mean ± SD	3512.4 ± 1523.4	2855.7 ± 1180.3	**0.71 (0.60–0.84, *p* = 0.022)**	
TILP	Mean ± SD	17.8 ± 22.8	15.0 ± 15.9	0.00 (0–7833.4, *p* = 0.401)		TILP	Mean ± SD	10.2 ± 14.0	11.3 ± 13.3	283.00 (29.48–2718.95, *p* = 0.676)	
ICP	Mean ± SD	4208.0 ± 1450.8	4571.6 ± 1201.5	1.19 (0.97–1.45, *p* = 0.097)	**1.820 (1.028–3.223, *p* = 0.040)**	ICP	Mean ± SD	4105.8 ± 1552.8	4505.6 ± 1187.3	1.00 (1.00–1.00, *p* = 0.159)	
Age	Mean ± SD	50.9 ± 12.1	45.6 ± 10.4	**0.96 (0.94–0.99, *p* = 0.005)**	**0.96 (0.92–1.00, *p* = 0.032)**	Age	Mean ± SD	49.6 ± 10.3	45.6 ± 11.0	0.96 (0.93–1.00, *p* = 0.053)	
Ki-67LI (%)	Mean ± SD	41.2 ± 28.7	74.0 ± 14.3	**1.06 (1.04–1.08, *p* < 0.001)**	**1.05 (1.02–1.07, *p* < 0.001)**	Ki-67LI (%)	Mean ± SD	39.2 ± 32.5	75.0 ± 14.3	**1.06 (1.03–1.09, *p* < 0.001)**	**1.07 (1.03–1.10, *p* < 0.001)**
Subtype	HER2 +	20 (7.4%)	1 (2%)			Subtype	HER2 +	8 (8.6%)	1 (2.6%)		
	HR +	130 (48.1%)	4 (8%)	0.62 (0.07–5.79, *p* = 0.671)			HR +	35 (37.6%)	3 (7.9%)	0.69 (0.06–7.48, *p* = 0.757)	
	HR + /HER2 +	30 (11.1%)	1 (2%)	0.67 (0.04–11.29, *p* = 0.779)			HR + /HER2 +	14 (15.1%)	1 (2.6%)	0.57 (0.03–10.43, *p* = 0.706)	
	TNBC	90 (33.3%)	44 (88%)	**9.78 (1.27–75.23, *p* = 0.028)**			TNBC	36 (38.7%)	33 (86.8%)	7.33 (0.87–61.82, *p* = 0.067)	
Diagnosis	IDC	250 (92.6%)	45 (90%)			Diagnosis	IDC	87 (93.5%)	34 (89.5%)		

Table 3 (continued)

Variable*		All (n = 320) Failure (n = 270)	Success (n = 50)	Univariate ** (Odds ratio, 95% CI, *p*-value***)	Multivariate ** (Odds ratio, 95% CI, *p*-value***)	Variable*		NAC group (n = 131) Failure (n = 93)	Success (n = 38)	Univariate ** (Odds ratio, 95% CI, *p*-value***)	Multivariate** (Odds ratio, 95% CI, *p*-value***)
	Other	20 (7.4%)	5 (10%)	1.39 (0.50–3.89, *p* = 0.532)			Other	6 (6.5%)	4 (10.5%)	1.71 (0.45–6.42, *p* = 0.430)	
HG	2	139 (51.5%)	3 (6%)			HG	2	41 (44.1%)	3 (7.9%)		
	3	131 (48.5%)	47 (94%)	**16.62 (5.05–54.71, *p* < 0.001)**	**4.34 (1.08–17.53, *p* = 0.039)**		3	52 (55.9%)	35 (92.1%)	**9.20 (2.64–32.05, *p* < 0.001)**	
NAC	No	177 (65.6%)	12 (24%)			Miller-Payne grade	Mean ± SD	2.3 ± 0.8	1.6 ± 0.8	**0.34 (0.20–0.57, *p* < 0.001)**	**0.30 (0.16–0.58, *p* < 0.001)**
	Yes	93 (34.4%)	38 (76%)	**6.03 (3.01–12.09, *p* < 0.001)**	**3.27 (1.41–7.60, *p* = 0.006)**	RCB score	Mean ± SD	3.1 ± 1.0	3.4 ± 1.2	1.24 (0.86–1.78, *p* = 0.253)	
Size (cm)	Mean ± SD	3.1 ± 2.0	4.4 ± 2.8	**1.23 (1.09–1.38, *p* < 0.001)**	**1.20 (1.02–1.41, *p* = 0.029)**	Size (cm)	Mean ± SD	4.0 ± 2.6	5.0 ± 2.9	1.13 (0.99–1.30, *p* = 0.064)	
LVI	No	151 (55.9%)	30 (60%)			LVI	No	44 (47.3%)	21 (55.3%)		
	Yes	119 (44.1%)	20 (40%)	0.85 (0.46–1.56, *p* = 0.594)			Yes	49 (52.7%)	17 (44.7%)	0.73 (0.34–1.55, *p* = 0.410)	
Metastatic LNs	Mean ± SD	2.1 ± 5.8	4.5 ± 9.5	**1.04 (1.00–1.08, *p* = 0.031)**		Metastatic LNs	Mean ± SD	4.1 ± 8.9	5.8 ± 10.6	1.02 (0.98–1.06, *p* = 0.350)	
TIL (%)	Mean ± SD	12.0 ± 18.4	9.4 ± 13.8	0.99 (0.97–1.01, *p* = 0.351)		TIL (%)	Mean ± SD	6.1 ± 11.6	6.3 ± 8.5	1.00 (0.97–1.04, *p* = 0.928)	

AP Adipose proportion, *NP* Necrosis proportion, *BP* Background proportion, *TDLUP* Terminal ductal lobular unit proportion, *SP* Stroma proportion, *TILP* Tumor-infiltrating lymphocyte proportion, *ICP* Invasive carcinoma proportion, *Ki-67LI* Ki-67 labeling index, *HR* + Hormone receptor-positive breast cancer, *TNBC* Triple-negative breast cancer, *HR* + */HER2* + Hormone receptor and HER2 positive breast cancer, *HER2* + HER2 positive breast cancer, *IDC* Invasive ductal carcinoma, *HG* Histologic grade, *NAC* Neoadjuvant chemotherapy, *LVI* Lymphovascular invasion, *LN* Lymph node, *TIL* Tumor infiltrating lymphocytes

* AP, BP, NP, TDLUP, SP, TILP, ICP values scaled up by 10,000

** AP, BP, NP, TDLUP, SP, TILP, ICP: OR calculated with 1,000-unit change, corresponding to 0.1% of intratumoral percentage adjustment

*** Bold: significant at *p*-value < 0.05

Table 4. Decision tree analysis with AI and clinicopathological factors in primary breast cancer group, including the chemo-naïve and NAC groups (n=320).

Parameter Value	Value
Number of Observations (n) 320	320
Method Classification	Classification
Complexity Parameters (CP) 0.08, 0.06	0.08, 0.06, 0.03, 0.01
Number of Splits (nsplit) 0, 2, 4, 6	0, 2, 4, 6
Relative Error 1.00, 0.84, 0.72, 0.66	1.00, 0.84, 0.72, 0.66
Cross-Validation Error (xerror) 1.00, 1.1	1.00, 1.18, 1.18, 1.14
Cross-Validation Std (xstd) 0.130, 0.13	0.130, 0.139, 0.139, 0.137

Variable Importance (%)*

Variable	Importance (%)
Subtype	20
Size	14
NP	13
Ki67LI	12
Age	7
SP	6
Metastatic LN	6
HG	6
TDLUP	5
LVI	2
ICP	2
AP	2

Node Information

Node No.	Obs.	P(node)	Class Counts (0/1)	Probabilities (0/1)	Expected Loss	Important Variables
1	320	1	270/50	0.844/0.156	0.15625	Subtype, Ki67LI, HG, NAC, NP
2	186	0.581	180/6	0.968/0.032	0.03226	
3	134	0.419	90/44	0.672/0.328	0.3284	size, NAC, Age,Ki67LI, metastatic LN
6	98	0.306	76/22	0.776/0.224	0.2245	Age, SP, Ki67LI, NP, BP
7	36	0.113	14/22	0.389/0.611	0.3889	NP, BP, TDLUP, Ki67LI, ICP
12	68	0.213	59/9	0.868/0.132	0.1324	
13	30	0.094	17/13	0.567/0.433	0.4333	SP, metastatic LN, TDLUP, BP, AP
14	22	0.069	12/10	0.545/0.455	0.4545	metastatic LN, BP, NP, AP, ICP
15	14	0.044	2/12	0.143/0.857	0.1429	
26	11	0.034	9/2	0.818/0.182	0.1818	
27	19	0.059	8/11	0.421/0.579	0.4211	
28	12	0.038	9/3	0.750/0.250	0.25	
29	10	0.031	3/7	0.300/0.700	0.3	

NP, necrosis proportion; *Ki67LI*, Ki-67 labeling index (%); *SP*, stroma proportion; *metastatic LN*, metastatic lymph node; *HG*, histologic grade; *BP*, background proportion; *TDLUP*, terminal ductal lobular unit proportion; *LVI*, lymphovascular invasion; *ICP*, invasive carcinoma proportion; *AP*, adipose proportion; *NAC*, neoadjuvant chemotherapy.

* Variable importance less than 1% were not described.

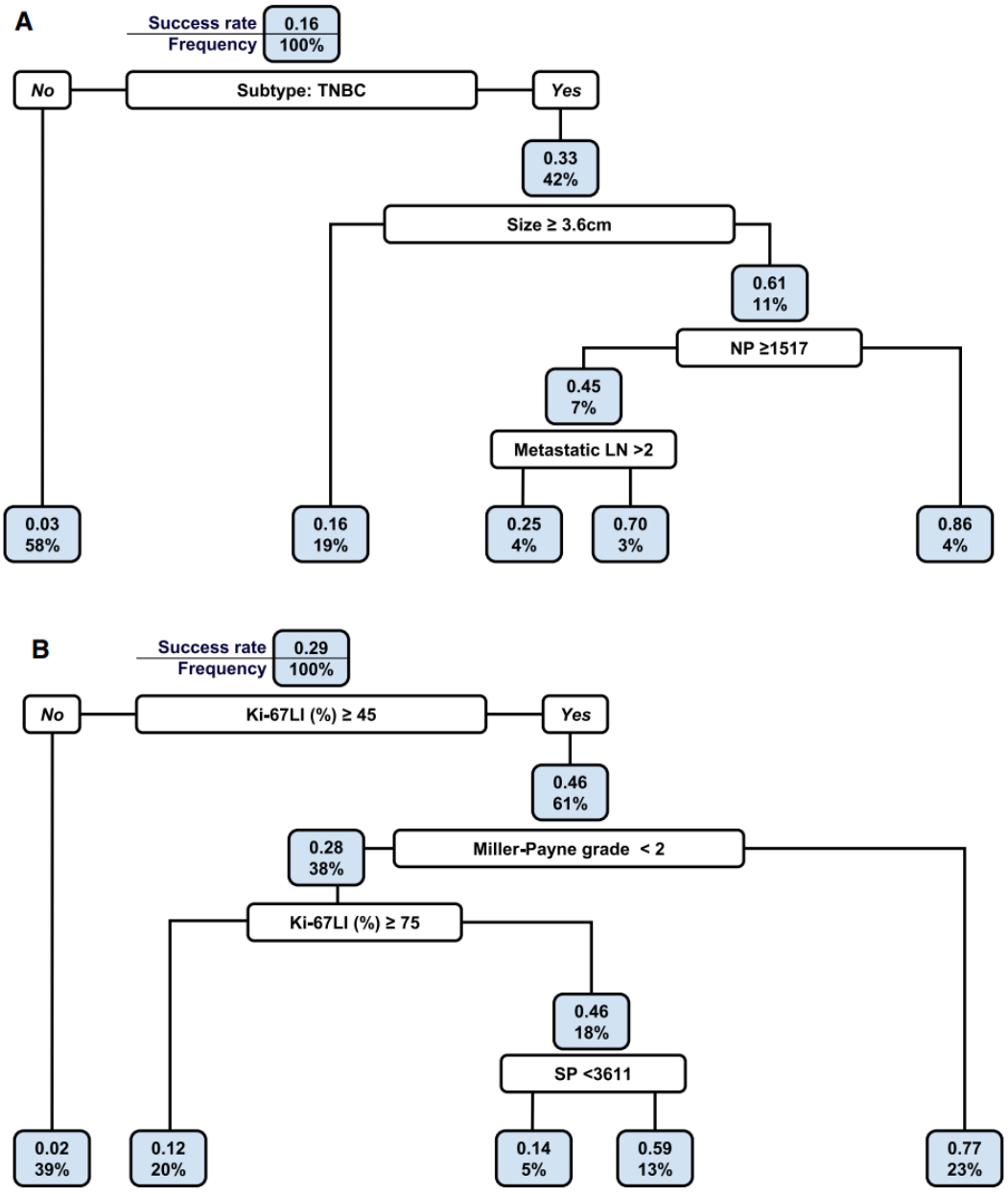

Figure 2.5. Pruned decision tree analyses

A. Primary breast cancer (n=320) and B. NAC-treated group (n=131).

2.4.2 Factors affecting the engraftment success rates of NAC-treated primary breast cancer

Separate statistical analyses were carried out for the NAC group with additional inclusion of unique variables, including the Miller-Payne grade, RCB class, and RCB score (Table 1). In the NAC group, samples from 47 of total 156 patients led to successful PDX engraftment (30.1%, 47/156). A significant difference was noted in the mean age between the failure and success groups, with younger age at diagnosis significantly related to PDX engraftment (50.4±10.7 vs. 45.2±11.0 years; p=0.007). The proportion of the TNBC subtype

was higher in the success group (87.2%) compared to the failure group (33.9%; p<0.001). Ki-67LI (%) displayed a significant elevation in the success group, registering at 74.0±15.1 compared to 33.9±32.3 in the failure group (p<0.001). The histologic grade also displayed a significant association with PDX engraftment success (p<0.001). Specifically, the successful cases featured a high prevalence of histologic grade 3, accounting for 91.5% (43 out of 47), in contrast to 49.5% (54 out of 109) in the failure group. No significant differences were detected in variables such as diagnosis, LVI, the number of positive LNs, TIL%, tumor size, or AJCC stages between the success and failure groups. The Miller-Payne grade was significantly associated with PDX success (p<0.001). While the RCB score did not show a significant difference, the RCB class showed a statistical trend toward success (p=0.052).

A cohort of 131 NAC-treated primary breast cancers were analyzed using AI-detected morphometric features. These morphometric features were compared between the failure (n=93) and success (n=38) groups (Table 2). A notable statistical significance was observed for NP, which was considerably higher in the success group (1642.8±1358.9 vs. 901.3±1101.4; p=0.001). TDLUP showed a significant decrease in the success group compared to the failure group (201.6±213.9 vs. 475.2±730.2; p=0.001). Similarly, SP was significantly lower in the success group (2855.7±1180.3 vs. 3512.4±1523.4; p=0.019).

Univariate and multivariate logistic regression analyses were conducted, incorporating both clinicopathologic factors and AI-analyzed intratumoral image patch data from 131 NAC-treated primary breast cancers (Table 3). In univariate analysis, higher Ki-67LI, histologic grade 3, and lower Miller-Payne grade were found to be significantly associated with PDX engraftment, with odds ratios (ORs) of 1.06 (95% CI 1.03-1.09, p<0.001), 9.20 (95% CI 2.64-32.05, p<0.001), and 0.34 (95% CI 0.20-0.57, p<0.001), respectively. For the morphometric features, higher NP, lesser TDLUP, and lesser SP were significantly associated with PDX engraftment. Specifically, a 0.1% increase in NP was associated with higher odds of successful engraftment (OR 1.60, CI 1.38-1.85, p=0.003), while 0.1% increase in, TDLUP and SP indicated a decreased chance of engraftment (OR 0.22, CI 0.18-0.27, p=0.034 and OR 0.71, CI 0.60-0.84, p=0.022, respectively).

In multivariate logistic regression analysis for the NAC group, the variables TDLUP, Ki-67LI, and Miller-Payne grades were selected as the variables that optimized the AIC. A higher Ki-67LI and lower Miller-Payne grade resulted in successful PDX engraftments with ORs of 1.068 (95% CI 1.034-1.102, p<0.001) and 0.303 (95% CI 0.158-0.577, p<0.001), respectively. A lesser TDLUP was associated with PDX success, with 0.1% increase in TDLUP yielding an OR of 0.998 (95% CI 0.033-1.000, p=0.062), showing a statistical trend.

To evaluate the robustness of the logistic regression model, a bootstrap analysis was conducted using 1000 samples. The original AUC was 0.889, with an associated 95% BCa confidence interval ranging from 0.8204 to 0.9348. The optimal cutoff value for the model, determined by Youden's J statistic, was 0.2863. At this cutoff, the PPV was 0.6034 and the

NPV was 0.9589 (Fig. 2C).

In the decision tree for the NAC group incorporating both AI-derived and clinicopathological factors, the tree was pruned at two different CPs, with the optimal CP being 0.0395 as determined by the lowest cross-validation error. The root node error was evaluated at 0.2901, based on 93 failures and 38 successes among the observations (Fig. 5B).

When assessing variable importance, Ki-67LI emerged as the most influential factor, contributing 22% to the model's predictive power. This was followed by Miller-Payne grade (13%), subtype (12%), SP (11%), and histologic grade (9%). Other variables like NP, size, RCB score, and ICP each contributed less than or equal to 5%, whereas variables like LVI, metastatic LNs, TILP, TIL, and age had minimal impact (Table 5).

The decision tree model for the NAC group demonstrated an AUC of 0.8967, with a bias of 0.0065 and a standard error of 0.0419. The BCa 95% confidence interval for the AUC ranged between 0.7680 and 0.9524 after bootstrapping with 1000 replicates. The recommended cutoff point based on Youden's J statistic was 0.2863, at which the model yielded a PPV of 0.6034 and an NPV of 0.9589 (Fig. 4D)

2.4.3 Engraftment success across sequential PDX passages and associated clinicopathological factors: metastatectomy cases (n=19)

The characteristics of the metastatic breast cancers in relation to the success of PDX engraftment are summarized in Table 6. A statistically significant difference was observed in the distribution of cancer subtypes between PDX engraftment success and failure groups (p=0.013). Specifically, all successful engraftments occurred for tumors with the TNBC subtype (4 out of 4, 100%) while none of the HR + cases (0 out of 11, 0%) or HR + /HER2 + cases (0 out of 1, 0%) were successful.

The distribution of histologic grade between the unsuccessful and successful PDX groups, although not reaching statistical significance (p=0.134), demonstrated a higher prevalence of grade 3 tumors in the success group at 75% (3/4) compared to 20% (3/15) in the failure group. Although the anatomical site of metastatectomy did not significantly impact PDX engraftment (p=0.207), the successful group displayed a more diverse distribution of metastasis sites: bone at 25% (1/4), axillary lymph nodes at 50% (2/4), and lung at 25% (1/4).

Table 5. Decision tree analysis with AI and clinicopathological factors in the NAC group (n=131).

Parameter	Value
Number of Observations (n)	131
Method	Classification
Complexity Parameters (CP)	0.21, 0.04, 0.01
Number of Splits (nsplit)	0, 2, 4
Relative Error	1.00, 0.58, 0.50
Cross-Validation Error (xerror)	1.00, 0.66, 0.89
Cross-Validation Std (xstd)	0.137, 0.118, 0.132

Variable Importance (%)*

Variable	Importance (%)
Ki-67LI	22
Miller-Payne grade	13
Subtype	12
Histologic grade	9
NP	7
Size	5
RCB score	5
ICP	5
LVI	3
Metastatic LN	2
TIL	2
Age	1

Node Information

Node No.	Obs.	P(node)	Class Counts (0/1)	Probabilities (0/1)	Expected Loss	Important Variables
1	131	1	93/38	0.710/0.290	0.2901	Ki-67LI, Miller-Payne grade, Subtype, Histologic grade, NP
2	51	0.39	18264	0.980/0.020	0.0196	
3	80	0.61	43/37	0.538/0.463	0.4625	Miller-Payne grade, RCB score, Size, NP, Ki-67LI
6	50	0.38	36/14	0.720/0.280	0.28	Ki-67LI, Age, SP, RCB score, NP
7	30	0.23	45130	0.233/0.767	0.2333	NP, TDLUP, Ki-67LI, ICP
12	26	0.2	45008	0.885/0.115	0.1154	
13	24	0.18	45243	0.542/0.458	0.4583	SP, Metastatic LN, TDLUP, ICP

Ki67LI: Ki-67 labeling index (%); *NP*: Necrosis proportion; *RCB*: Residual Cancer Burden; *ICP*, invasive carcinoma proportion; *LVI*: lymphovascular invasion; *LN*: lymph node; *TIL*: tumor infiltrating lymphocytes' *SP*: Stroma proportion; *TDLUP*: terminal ductal lobular unit proportion

* Variable importance less than 1% were not described.

Table 6. Characteristics of the metastatic breast cancer group affecting the success of PDX engraftment (n=19)

Variable	Failure (n=15)	Success (n=4)	p-value
Subtype			0.013
- HR+	11 (73.3%)	0 (0.0%)	
- HR+/HER2+	1 (6.7%)	0 (0.0%)	
- TNBC	3 (20.0%)	4 (100.0%)	
Histologic Grade			0.134
- Grade 2	12 (80.0%)	1 (25.0%)	
- Grade 3	3 (20.0%)	3 (75.0%)	
Site of Metastasis			0.207
- Bone	9 (60.0%)	1 (25.0%)	
- Liver	3 (20.0%)	0 (0.0%)	
- Axillary LN	2 (13.3%)	2 (50.0%)	
- Lung	1 (6.7%)	1 (25.0%)	

HR+, hormone receptor-positive breast cancer; *TNBC*, Triple-negative breast cancer; *HR+/HER2+*, hormone receptor and HER2 positive breast cancer; *HER2+*, HER2 positive breast cancer; *HG*, histologic grade; *LN*, lymph node

*Bold: significant at P < .05.

2.5 Discussion

Previous studies on PDX have focused on clinicopathologic or technical parameters for predicting the success of PDX engraftment. In this study, we found that higher Ki-6LI, younger age at diagnosis, NAC treatment status, larger tumor size, and higher proportions of intratumoral necrosis and invasive carcinoma (as quantified by AI) were significant variables predictive of PDX engraftment success.

Our findings revealed that high Ki-67LI, a marker of cellular proliferation, was a crucial factor for successful PDX engraftment (32,34,35). This finding is consistent with previous studies that linked high histologic grade and TNBC subtype, which are often associated

with elevated Ki-67LI, to increased PDX engraftment rates (11,13,14,36,37). These tumors, particularly prevalent in younger patients, reportedly exhibit aggressive behavior and high cancer stem cell (CSC) levels (38,39).

Increased PDX engraftment rates in the NAC group were also noted in current study. NAC, involving cytotoxic agents, seemed to select cancer cells with survival traits which would largely include CSCs, resistant to NAC due to their ability to evade reactive oxygen species and their non-proliferative nature, as suspected by Diehn and Phi et al (40,41). Substantiating the allegations, post-NAC breast cancer cells showed genetic markers associated with CSCs and high tumorigenic potential in a study by Creighton et al (42). Moreover, NAC was observed to modify the tumor microenvironment, including the vascular architecture, which may enhance tumor growth (34). However, the impact of NAC on PDX engraftment rates in breast cancer remains a subject of debate in the scientific literature. McAuliffe et al (15) found a significantly higher PDX engraftment rate in the NAC group at 41.7% (10/24) versus 8.3% (2/24) in the chemo-naïve group (p=0.02). Furthermore, in the same study, within the NAC group, patients with progressive disease exhibited higher engraftment rates (85.7%, 6/7) compared to those with a stable or partial response (29.4%, 5/17). However, Goetz et al. (13) found no significant difference in engraftment success between the NAC group and the chemo-naïve group. Cottu et al. (11) also did not find preoperative treatment to significantly influence engraftment success. Thus, factors affected the success of post-NAC cancer PDX grafts should be further evaluated.

While some studies have indicated that metastatic cancers generally have higher PDX engraftment rates compared to their nonmetastatic counterparts (35,43), the success rate of PDX engraftment of breast cancer according to region of harvest remains a subject of ongoing debate. Cottu et al. (11) reported higher engraftment success rates with primary breast tumors compared to metastatic samples, while conversely, Marangoni et al. (14) observed increased engraftment success with samples of metastatic origin. Given the limited number of studies comparing primary to metastatic tumors, further research is essential to clarify the role of tumor origin in PDX engraftment success rates. This will provide more comprehensive insights into the factors predictive of successful PDX modeling.

Despite the valuable insights provided by our study, we acknowledge several limitations. Our AI model faced challenges in differentiating between IDC and DCIS due to the small patch size utilized, requiring manual intervention. Furthermore, the model struggled to distinguish between invasive lobular carcinoma, scattered histologic grade 2 IDCs, stromal components, and TDLU. These limitations could be addressed in future studies by using larger patches and more sophisticated machine learning techniques. Our approach acknowledges the inherent challenges of integrating machine learning techniques with

histopathology (15). The histopathological complexity and subtle invasion patterns of invasive lobular carcinoma present challenges even for experienced pathologists (41, 44). These limitations could be addressed in future iterations of our model through the utilization of a larger dataset that encompasses finer patterns of invasive carcinomas and by integrating more sophisticated machine learning techniques.

Our study has shown that the incorporation of specific clinicopathological variables and morphometric features can effectively predict PDX engraftment. The efficacy of our multivariate logistic regression model (AUC=0.905) is excellent. Additionally, the statistical analysis of the NAC group, which included TDLUP, Miller-Payne grade, and Ki-67LI in the multivariate logistic regression analysis, also demonstrated an excellent predictive ability with an AUC of 0.89. Compared to the PDX graft studies in the literature, our score was higher than that reported by Echeverria et al. who incorporated two variables, Ki-67LI and metastatic LNs, into a logistic regression model for TNBCs breast PDX survival (AUC 0.70) (35). In the same context, Zhuo et al. (45) used GPC3 expression and KI67LI to predict hepatocellular carcinoma PDX engraftment and found a good discriminatory power (AUC 0.828), which is similar to the score obtained in the current study. Our study also effectively selected a few variables in a parsimonious manner for predicting PDX engraftment.

Chapter 3. PDX engraftment success factors in the literature

3.1 Abstract

PDXs have emerged as a valuable tool for cancer research, enabling the study of tumor biology and the evaluation of novel therapeutic strategies. However, the success of PDX engraftment varied widely depending on various factors. This literature review aimed to identify and summarize the key factors influencing PDX engraftment success across different tumor types, with a specific focus on breast cancer.

A comprehensive literature search was conducted using PubMed, Embase, and Web of Science databases. Studies reporting PDX engraftment success rates and associated factors were included in the analysis. The reviewed studies encompassed a diverse range of tumor types and experimental conditions.

The choice of mouse strain significantly impacted PDX engraftment success, with immunodeficient strains such as NOD/SCID and NSG mice demonstrating higher engraftment rates compared to nude mice. Orthotopic implantation generally resulted in higher success rates than heterotopic implantation. Engraftment rates varied widely across tumor types, with brain tumors exhibiting the highest success rate (69%) and breast cancer rates ranging from 2.5% to 90%.

In breast cancer, ER-negative tumors and those with a higher histologic grade (grade 3) showed higher engraftment rates. The method of engraftment also influenced success, with intraductal injection yielding the highest take rate (77%). The relationship between tumor origin (primary or metastatic) and engraftment success remained inconclusive, with conflicting findings across studies.

This review highlighted the complex interplay of factors influencing PDX engraftment success and underscored the need for careful consideration of these variables in the design and interpretation of PDX studies. Further research is warranted to optimize PDX models and enhance their translational value in cancer research.

3.2 Introduction

The success of PDX engraftment varies significantly depending on a multitude of factors. These factors include the choice of mouse strain, implantation site, tumor type and subtype, histologic grade, and various experimental conditions. Understanding the impact of these factors on PDX engraftment success is crucial for the optimal design and interpretation of PDX-based studies. Moreover, identifying the key determinants of engraftment success could help researchers to develop strategies

for improving the efficiency and reliability of PDX models.

This literature review aimed to provide a comprehensive overview of the factors influencing PDX engraftment success across different tumor types, with a particular emphasis on breast cancer. By synthesizing the findings from multiple studies, we sought to shed light on the complex interplay of variables that shaped the outcome of PDX engraftment. The insights gained from this review could inform future efforts to optimize PDX models and enhance their translational value in cancer research.

3.3 Methods

3.3.1 Literature search strategy

A comprehensive literature search was conducted to further delineate the factors impacting PDX engraftment. The search was conducted using electronic databases including PubMed, Embase, and Web of Science, with the search terms "PDX", "patient-derived xenografts", "engraftment", “take rate”. The search was limited to articles published in English up to March 2023.

3.3.2 Inclusion and exclusion criteria

Inclusion criteria for this review were defined as articles that reported factors influencing the success of PDX engraftment. Articles lacking explicit engraftment success rates or well-defined methodology were not considered for this review. Further, the focus was primarily on studies using animal models, predominantly mice, with one notable exception (chick chorioallantoic membrane) for PDX engraftment. The data extracted from the included articles spanned various parameters, such as engraftment take rates, histologic grades, tumor types, NAC groups, engrafted mice strains, engraftment methods, utilized supplements, and distinctions between primary and metastatic origins.

3.4 Results

3.4.1 Determinants of PDX engraftment success across different studies

We reviewed the literature on factors affecting the success of PDX engraftment, and 89 PDX studies were identified through web search. Our analysis included a range of tumor types, mice strains, and implantations sites, as summarized in Table 7.

Table 7. PDX engraftment information in the literature.

Tumor Type	Mice Strain	Implantation Site	Number of Sample	Engraftment Ratio	References
Brain	NOD/SCID	s.c.*	16	69%	Zeng, 2020
Breast cancer	Nude	s.c.	200	13%	Marangoni, 2007
	Nude	fat pad**	423	8%	Cottu, 2012
	NOD/SCID	fat pad	49	27%	DeRose, 2011
	SCID/Beige, NSG	s.c.	169	41%	Zhang, 2013
	NSG	intraductal injection	31	77%	Richard, 2016
	Nude	s.c.	48	27%	McAuliffe, 2015
	NOD/SCID&NSG	s.c.	113	27%	Yu, 2017
	NOD/SCID&NSG	s.c.	113	27%	Goetz, 2017
Cholangiocarcinoma	SCID	s.c.	55	35%	Ojima, 2010
	NOD/SCID	s.c.	20	6%	Cavalloni, 2016
	BRJ	s.c.	16	75%	Vaeteewoottacharn, 2019
Colorectal cancer	Nude	s.c.	85	64%	Julien, 2012
	NOD/SCID	s.c.	85	87%	Bertolini, 2011
	NSG	s.c.	27	54%	Chou, 2013
	NSG	s.c.	44	64%	Wimsatt, 2018
	Nude	s.c.	35	43%	Fichtner,2004
	Nude	s.c.	26	77%	Dangles-Marie,2007
	SCID/beige	s.c.	10	60%	Mischek,2009
	NOD/SCID and Nude	s.c.	48	72%	Linnebacher,2010
	Nude	s.c.	60	NA	Jin,2011
	NOD/SCID	s.c.	20	70%	Kim,2012
	NOD/SCID	s.c.	18	50%	Monsma,2012
	NOD/SCID	s.c. or orthotopic	40	88%	Puig,2013
	NOD/SCID and Nude	s.c.	10	100%	Lee,2014
	Nude	s.c.	241	62%	Oh, 2015
	Nude	s.c.	85	59%	Guan, 2016
	Nude	s.c.	37	54%	Cybulska, 2018
	NOG	s.c.	48	73%	Fuji, 2015
	NSG	s.c.	90	56%	Katsiampoura, 2017
Endometrial cancer	Nude	s.c.	143	67%	Cho,2014
	Nude	s.c.	40	60%	Depreeuw, 2015
	Nude	s.c.	32	74%	Wang, 2017
Gastric cancer	NOD/SCID	s.c.	185	34%	Zhu, 2015
	Nude	s.c.	83	17%	Zhang, 2015
	NOD/SCID	s.c.	119	27%	Zhang, 2015
	Nude/NOG	s.c.	62	24%	Choi, 2016
Glioblastoma (WHO grade IV glioma)	NSG	orthotopic	100	30%	Brabetz, 2018
	Nude	s.c.	261	36%	Vaubel, 2020
Gynecologic and breast cancer	Nude	s.c.	36	66%	Murata, 2020
	Nude	s.c.	7	14%	
Head and neck cancer	Nude	s.c.	46	54%	Keysar, 2013
	NSG	s.c.	62	48%	Klinghammer, 2017
	NSG	s.c.	34	79%	Swick, 2017
	NSG	s.c.	115	45%	Klinghammer, 2015
Leukemia	NSG	s.c.	26	85%	Kimple, 2013
	NOD/SCID&NSG	ntravenous) or via the femu	127	65%	Alruwetei, 2020
	NSG	tail vein (intravenous)	29	59%	Vick, 2015
Melanoma	NOG	s.c.	26	88%	Einarsdottir, 2014
	chick chorioallantoic m	chick chorioallantoic membrane	46	80%	Tsimpaki,2023
	NSG	s.c.	694	66%	Krepler, 2017

Multiple origin	NOD/SCID	s.c.	436	17%	Fujii, 2008
	Nude	s.c.	22	86%	Pauli, 2017
	NOD/SCID	s.c.	102	25%	Fichtner, 2008
	NOD/SCID	r.c.***	527	90%	Dong, 2010
	NOD/SCID	s.c.	308	26%	Chen, 2019
	NSG	s.c.	441	29%	Wang, 2017
Non-small lung cancer	SOH,NOD	s.c.	33	33%	Ktia, 2019
	NOD/SCID	s.c.	157	40%	John, 2011
	NOD/SCID	unstated	33	6%	Stewart, 2015
	SCID&nude	s.c.	97	39%	Moro, 2017
	SCID&nude	s.c.	100	35%	Ilie, 2015
	NOD/SCID	fat pad	12	67%	Anderson, 2015
	NOD/SCID	s.c.	75	49%	Chen, 2021
	Nude	s.c.	138	25%	Ricci, 2014
	Nude	r.c.	45	49%	Heo, 2017
	SCID	s.c.	34	50%	Dobbin, 2014
	SCID	s.c.	168	74%	Weroha, 2014
	NSG	s.c.	12	83%	Topp, 2014
Ovarian cancer	Nude	inter-scapular fat pad	66	74%	VoluColombo, 2015
	Nude	Intraperitoneal	94	31%	Liu, 2017
	SCID	Intraperitoneal	245	74%	Karlan, 2014
	NOD/SCID	s.c.	66	68%	Alkema, 2015
	SCID	Intraperitoneal	245	74%	Weroha, 2014
	humanized NBSGW	Intraperitoneal	9	67%	Steinkamp,2023
	NOD/SCID	r.c.	11	100%	Lee, 2005
	Nude	s.c.	69	61%	Garrido-Laguna, 2011
	SCID	s.c.	12	67%	Mattie, 2013
	Hsd:athymic nude-Foxn	orthotopic	35	43%	Choi, 2019
Pancreatic cancer	Nude	intraperitoneal	unspecified	58%	Rubio-Manzanare, 2018
	Nude	s.c.	unspecified	70%	
	Nude	orthotopic	unspecified	55%	
	NSG	s.c.	121	71%	Guo, 2019
	Nude	s.c.	23	39%	Priolo, 2010
	NOD/SCID	s.c.	23	48%	
	SCID	s.c.	86	58%	Wang, 2005
	SCID	orthotopic	57	72%	
Prostate cancer	SCID	r.c.	122	93%	Toivanen, 2011
	NOD/SCID	r.c.	41	41%	
	NOD/SCID	r.c.	38	66%	
	NOD/SCID&NSG	r.c.	10	70%	Lawrence, 2015
	NSG	s.c.	27	37%	Wetterauer, 2015
	Nude	s.c.	336	9%	Lang, 2016
	NOD/SCID	r.c.	94	37%	Sivanand, 2013
Renal cell carcinoma	NSG, NMRI nu/nu	s.c.	4	25%	Jang, 2016
	NSG	s.c.	74	45%	Dong, 2017
	Nude	s.c.	12	58%	Keysar, 2018
Salivary gland cancer	NOD/SCID	s.c.	68	44%	Castillo-Ecija, 2021
Sarcoma	NOD/SCID	r.c.	14	71%	Larmour, 2018
Uterine cervix cancer	Nude	r.c.	21	67%	Oh, 2015

* subcutaenous, ** axillary fat pad ***subrenal capsule

3.4.2 Mouse strains and engraftment success

As for host strains, a range of mice strains and chick chorioallantoic membrane from one melanoma study were included. The chick chorioallantoic membrane had the highest success rate with 78.3% (36 successful out of 46 attempts) (46). As for mice strains, NOG strain at 77.0% (57 successful out of 74 attempts), and NOD/SCID and Nude at 75.9% (44 successful out of 58 attempts) showed highest engraftment rates. Other strains, such as BRJ and SCID, also had high success rates of 75.0% (12 successful out of 16 attempts) and 71.4% (731 successful out of 1024 attempts), respectively. Strains including NSG and NOD/SCID demonstrated moderate success rates of 52.0% (1018 successful out of 1959 attempts) and 46.5% (1188 successful out of 2557 attempts), respectively. However, strains

like Hsd:athymic nude-Foxn1 and NOD/SCID&NSG showed success rates of less than 50%, with 42.9% (15 successful out of 35 attempts) and 41.0% (149 successful out of 363 attempts), respectively. The strains with the lowest success rates included Nude/NOG and SCID/Beige, with success rates of 24.2% (15 successful out of 62 attempts) and 20.9% (36 successful out of 172 attempts), respectively (11-20,36).

3.4.3 Tumor types and engraftment success

The type of tumor also played a significant role in the success of PDX engraftment. High success rates were noted in colorectal cancer at 65.3% (752 successful out of 1152 attempts), (47-67) melanoma at 67.1% (514 successful out of 766 attempts) (46,68), pancreatic cancer at 62.6% (214 successful out of 342 attempts) (69-73), and ovarian cancer at 62.2% (705 successful out of 1133 attempts)(74-77). Additionally, brain and uterine cervix tumors also displayed high success rates at 68.7% (11 successful out of 16 attempts) and 66.7% (28 successful out of 42 attempts), respectively (78).

On the other hand, tumor types such as breast cancer and multiple origin showed lower success rates of 17.6% (206 successful out of 1171 attempts) and 19.9% (91 successful out of 458 attempts), respectively (11,13-15,17,19,21,35,36,38,65,79,80). Intermediate success rates were seen in non-small lung cancer at 47.4% (894 successful out of 1885 attempts) (28,51,81,82,82,83), prostate cancer at 40.2% (307 successful out of 763 attempts) (84-88), and renal cell carcinoma at 40.2% (74 successful out of 184 attempts)(89-92)

3.4.4 Impact of implantation site

The site of implantation also significantly influenced the success of PDX engraftment. The subrenal capsule site showed the highest success rate of 77.9% (752 successful out of 965 attempts), followed by intraductal injection with a success rate of 74.2% (23 successful out of 31 attempts), and inter-scapular fat pad at 72.7% (48 successful out of 66 attempts). Sites such as Intraperitoneal and lateral tail vein (intravenous) or via the femoral artery (intra-arterial) showed success rates of 66.9% (397 successful out of 593 attempts) and 64.6% (82 successful out of 127 attempts) respectively. Lower success rates were observed at the orthotopic site with 45.8% (104 successful out of 227 attempts) and the fat pad site with 11.2% (54 successful out of 484 attempts).

3.4.5 Comparative analysis from multiple studies on factors influencing engraftment success in breast PDX models

Eight breast cancer PDX studies with unambiguous mention of engraftment success rates were further evaluated (Table 8). Distinct factors influencing the success rate were analyzed. The studies included in the analysis span from Marangoni et al. to Goetz et al.

(13,14). The highest success rate was observed in the study by Richard et al. (16) with 77% (24 out of 31), while the lowest was reported by Cottu et al. (11) at 8% (35 out of 423).

Table 8. Comparative analysis of factors influencing engraftment success in breast PDX models across multiple studies

Study	PDX engraftment rate	Histologic grade	Tumor Type (Engraftment rate)
Richard, 2016	77% (24/31)	Grade 2 (13/14,93%)> Grade 3(10/15,67%) > Grade 1(1/2,50%)	Molecular apocrine (3/3, 100%) > Luminal A (6/8, 75%), Luminal B (15/20, 75%)
Zhang, 2013	41% (69/169)	Grade 3 (16/44, 37%) > Grade 2 (0%, 0/21) or Grade 1 (0%, 0/4) (Conditon 2, Estradiol supplemented SCID/Bg) Grade 2 (2/7, 29%) > Grade 3 (4/22, 18%) > Grade 1, No data (Condition 4, Unmanipulated NSG) Grade 3 (1/25, 4%) > Grade 2 (0/8, 0%) OR Grade 1 (0/5, 0%) (Condition 1, Unsupplemented SCID/Bg): Grade 3 (1/17, 5.9%) > Grade 2 (0/10, 0%) or Grade 1 (0/2, 0%), (Condition 3, Estradiol and fibroblast supplemented SCID/Bg)	ER -(~52%,15/29) > PR- (~37%,15/40) > > PR + (~9%,1/11)> ER+ (~2%,1/41)
DeRose, 2011	27% (12/49)	Not included	1. No significant correlation between ER, PR, or HER2 status (Fischer's exact test; ER or PR (p = 0.99) or HER2 status (p = 0.25)) 2. TNBC grew fastest
Cottu, 2012	8% (35/423)	High Ellis-Elston histological grade, and/or a high mitotic count (OR=10.04, P=0.052)	1. ER- (24.7%) > ER + (2.5%) (p<0.001). 2. TNBC (36.1%) >non-TNBC (4.1%) (p<0.001) 3. ER- status (OR=0.14, P=0.001)
Marangoni, 2007	12.5 % (25/200)	Grade 3 (30%, 22/74) >Grade 2 (11%, 8/75) >Grade 1 (3%, 1/34)	ER - (37%,19/52) > ER + (4%,5/125)
McAuliffe, 2015	27 % (13/48)	Not included	TNBC > HR+ (53.8%, 7/13 vs. 15.6%,5/32, p = 0.02)
Yu, 2017	25% (37/148)	Grade 3 > Grade 1-2 tumors (p = 0.0003; difference = 46.6%; 95% CI: 29.9–63.3%)	1. Clinical molecular subtype (p < 0.001): TNBC (51.3%; 20/39) > HER2+ (26.5%; 9/34) > Luminal B (5.0%; 2/40) > Luminal A (0%; 0/3) 2. TNBC > HER2+ (p = 0.0348; difference = 24.8%; 95% CI: 3.2–46.4%
Goetz, 2017	27.4% (31/113)	Not included	TNBC (20/39, 51.3%) > ER-/HER2+ (5/20, 25.0%) > ER+/HER2+ (4/14, 28.6%) > Luminal B (2/30, 6.7%) > Luminal A (0/9, 0%), Luminal unknown (0/1, 0%)

Table 8. Comparative analysis of factors influencing engraftment success in breast PDX models across multiple studies (continued)

Study	NAC group	Engrafted Mice Strain	Supplement
Richard, 2016	Not specified	NSG	oestradiol pellet, subcutaenous (ER + tumors)
Zhang, 2013	Some matched pre-and post-treatment samples, not specified	Condition 2: SCID/Bg with estradiol supplement (21%, 15/70) > Condition 4: NSG mice with estradiol supplement (19%, 6/32) > Condition 3: SCID/Bg mice with estradiol and immortalized normal human fibroblasts (3%,1/29) >Condition 1: Unmanipulated SCID/Bg (3%,1/38)	
DeRose, 2011	All chemo-naïve	NOD-SCID	Interscapular estrogen pellets (ER + tumors)
Cottu, 2012	Preoperative treatement did not have significance for engraftment (13.3%of total patient ,54/423)	Nude	E2 in drinking water
Marangoni, 2007	16% post-treatment, not specified with graft success rate	Nude	Estrogen in drinking water
McAuliffe, 2015	1. NAC group vs chemo naive group (10/24, 41.7% vs 2/24, 8.3%, p = 0.02). 2. NAC group with progressive disease (85.7%,6/7) > NAC group with stable or partial response (29.4%, 5/17)	BALB/c nu/nu	Not discussed
Yu, 2017	1. Pre-treatment percutaneous biopsies (27.4%, 31/113) > Post-NAC surgical samples (17.1% ,6/35) 2. Pre-treatment percutaneos biopsies with confirmed residual disease, Pre-treatment percutaneos biopsies with confirmed pathological complete remission:No significant differences TNBC (9/17 vs. 11/22; p = 0.999), HER2+ tumors (7/17 vs. 2/15; p = 0.2401)	NSG >NOD-SCID (p = 0.0012; difference = 39.9%; 95% CI: 17.7–62.0%)	17β-estradiol
Goetz, 2017	NAC group PDX success rate (17.1%, 6/35) not significantly better than chemo-naïve	NOD-SCID or NSG mice	17β-estradiol (water fed)

Table 8. Comparative analysis of factors influencing engraftment success in breast PDX models across multiple studies (continued)

Study	Manner of Engraftment (Engraftment rate)	Primary/Metastatic Origin	Additional factors
Richard, 2016	Intraductal injection with vectors (24/31 , 77%)[a] > Subcutaneous (0/26, 0%)	All primary breast tumor	Diagnosis: Other type(2/2)>IDC (16/22, 73%)>ILC(4/7, 57%) Age group: >55years (12/15,80%) > 45-55years (10/13, 77%) > <45years (2/3, 67%)
Zhang, 2013	Orthotopic (cleared mammary fat pad)	1. Mostly primary breast cancer 2. Pleural effusion, ascites were included but not stastically evaluated	
DeRose, 2011	Orthotopic (cleared mammary fat pad)	Primary or metastasis source did not significantly predict successful engraftment (Fisher's exact test, P = 0.09)	1. Mesenchymal stem cells (MSCs) increased tumor growth in three tested lines (two ER-and one ER+ line). 2. Shorter survival of patients was related to PDX engraftment success (p=0.02, log-rank statistics)
Cottu, 2012	s.c. (interscapular fat pad)	Primary (Take rate 9%, 35/369) >Metastastic (Take rate 0%, 0/54)	
Marangoni, 2007	s.c. (interscapular fat pad)	Metastatic origin (24%, 8/34) > Primary tumors (15%, 25/164)	1. Ductal carcinoma (18%, 28/152) > lobular carinoma (8%, 2/25) 2. Tumor size, lymph node invovlement was not associated with engraftment
McAuliffe, 2015	s.c. (left and right mid-back)	All primary breast tumor	PDX engraftment was related to lower recurrence-free survival (p = 0.015) and overall survival (p<0.001)
Yu, 2017	s.c.	All primary breast tumor (percuntaneous needle biopsy, surgical specimen)	
Goetz, 2017	Subcutaneous (flank)	All primary breast tumor (percuntaneous needle biopsy, surgical specimen)	

3.4.5.1 Histologic grade

Across several studies with documented data on histologic grades, there was a trend of increased PDX engraftment success associated with higher histological tumor grades. For instance, in the study by Richard et al. (16), Grade 2 tumors showed a higher engraftment rate of 93% (13/14) compared to Grade 3 tumors which had a rate of 67% (10/15).

Similarly, Marangoni et al. (14) reported a higher PDX engraftment rate for Grade 3 tumors at 30% (22/74) compared to Grade 2 tumors at 11% (8/75) and Grade 1 tumors at 3% (1/34).

This trend was also evident in the data from Zhang et al. (93) where under certain experimental conditions, Grade 3 tumors exhibited the highest engraftment rates. This was particularly notable under Condition 2 (Estradiol supplemented SCID/Bg) where Grade 3 tumors had an engraftment rate of 37% (16/44) as compared to no engraftment observed for Grade 2 or Grade 1 tumors. Moreover, Yu et al. (17) found a significantly higher PDX engraftment rate for Grade 3 tumors compared to Grades 1-2 tumors, a difference of 46.6% with a confidence interval of 29.9-63.3% (p=0.0003). Similarly, in the Cottu et al. (11) study, a high Ellis-Elston histological grade corresponded to a higher likelihood of successful PDX engraftment (OR=10.04, P=0.052).

3.4.5.2 Hormonal status of breast tumors

Tumor type has been consistently shown to influence the engraftment success in PDX models. ER- tumors generally demonstrated higher engraftment rates compared to their ER+ counterparts. In Zhang et al. (93), the PDX engraftment rate was notably higher in ER- tumors at approximately 52% (15/29) compared to just 2% (1/41) in ER+ tumors. Similarly, in the study by Marangoni et al. (14), the engraftment rate for ER- tumors was substantially higher at 37% (19/52), compared to a significantly lower rate of 4% (5/125) in ER+ tumors.

In Cottu et al. (11), the ER- tumors displayed a considerable PDX engraftment rate of 24.7% while the ER+ tumors had an engraftment rate of only 2.5% ($p<0.001$).

Meanwhile, TNBC showed high engraftment rates in several studies. For instance, in McAuliffe et al. (15) and Goetz et al. (2017), TNBC exhibited PDX engraftment rates of 53.8% (7/13) and 51.3% (20/39) respectively, outperforming hormone receptor-positive (HR+) tumors in each study. However, it's important to note that not all studies found significant differences based on ER status. For instance, DeRose et al.(12) found no significant correlation between ER, PR, or HER2 status and PDX engraftment success. These findings indicated a potential trend toward higher PDX engraftment success in ER- tumors, particularly TNBC, compared to ER+ tumors.

3.4.5.3 Impact of neoadjuvant chemotherapy (NAC)

In the reviewed studies, the impact of NAC on PDX engraftment rates appeared to vary, or some did not consider it as a statistically deserving factor. However, McAuliffe et al. (15) found a significantly higher PDX engraftment rate in the NAC group at 41.7% (10/24) versus 8.3% (2/24) in the chemo-naïve group (p=0.02). Furthermore, in the same study

within the NAC group, patients with progressive disease exhibited higher engraftment rates (85.7%, 6/7) compared to those with stable or partial response (29.4%, 5/17). Goetz et al. (13) also found no significant difference in engraftment success between the NAC group and the chemo-naïve group, with the NAC group's PDX success rate reported at 17.1% (6/35).

In contrast, Cottu et al.(11) did not find preoperative treatment to significantly influence engraftment success, even though NAC-treated group accounted for 13.3% (54/423) of total patients. From a slightly different point of view, Yu et al. (17) compared PDX engraftment rates between pre-treatment percutaneous biopsies (27.4%, 31/113) and post-NAC surgical samples (17.1%, 6/35), indicating a higher engraftment rate for the pre-treatment samples. Notably, there was no significant difference in engraftment success was when comparing pre-treatment percutaneous biopsies from the patients with confirmed residual disease after NAC versus those with pathological complete remission in TNBC (9/17 vs. 11/22; p=0.999) and HER2+ tumors (7/17 vs. 2/15; p=0.2401).

3.4.5.4 Mouse strain

Regarding the engrafted mouse strain, our review indicated notable variability across the studies and their influence on the engraftment success rate of PDX models. Specifically, the strains of engrafted mice used in the studies were varied, including NSG (13,16,17,93), SCID/Bg (36), NOD-SCID (13,94), Nude (11,14), and BALB/c nu/nu (15). In the analysis of the selected studies, PDX engraftment success rates varied among different mouse strains. The NSG mouse strain yielded the highest success rate in some studies. Richard et al.(16) reported an engraftment success rate of 77% (24/31) using NSG mice, the highest among all the studies analyzed. Additionally, Yu et al. (2017) found a significantly higher success rate in NSG mice (25%, 37/148) compared to NOD-SCID mice, emphasizing the potential advantage of the NSG strain.

NOD-SCID mice also demonstrated relatively high engraftment rates. DeRose et al. (12) and Goetz et al.(13) both achieved a success rate of 27% (12/49 and 31/113 respectively) using the NOD-SCID strain. However, Nude mouse strain had generally lower engraftment success rates. Cottu et al. (11) observed an 8% success rate (35/423) in Nude mice, while Marangoni et al. (14) reported a 12.5% (25/200) success rate. The BALB/c nu/nu strain was only utilized in one of the analyzed studies, with McAuliffe et al. (15) achieving a 27% (13/48) success rate.

3.4.5.5 Estradiol supplementation

In addition, the use of supplements, specifically estradiol, varied across studies and showed different effects on engraftment rates. Richard et al., 2016; Zhang et al., 2013;

Cottu et al., 2012; Marangoni et al., 2007; and Goetz et al., 2017 (11,13,14,16,36) all used estradiol as a supplement in their studies. However, there were disparities in the administration methods and the specific subsets of tumors they were used on (e.g., ER+ tumors), which could potentially influence the engraftment rates. For instance, in the study by Zhang et al., 2013, the engraftment success was notably different under various conditions where SCID/Bg mice were used with estradiol supplement, ranging from 21% (15/70, Condition 2) to 3% (1/29, Condition 3) where SCID/Bg mice with estradiol and fibroblast supplement (36).

The success rates of patient-derived xenograft (PDX) engraftment were also found to vary in relation to the use of estradiol supplements across the selected studies. Drawing from Zhang et al. (36), an estradiol supplement was associated with enhanced PDX engraftment success; The SCID/Bg mice supplemented with estradiol saw an engraftment success rate of 21% (15/70), significantly higher than the unsupplemented SCID/Bg group's 3% (1/38) rate.

However, other studies were ambiguous for estrogen effect on PDX survival alone, because there were no control mice group for comparison. In the study conducted by Richard et al. (11), subcutaneous estradiol pellets were used, yielding the highest engraftment success rate of 77% (24/31); however, the result may have been largely due to other variables. DeRose et al. (12) also used estradiol in the form of interscapular pellets, resulting in a PDX engraftment success rate of 27% (12/49). Yu et al. (17) and Goetz et al. (13) both administered 17β-estradiol, observing a success rate of 25% (37/148) and 27.4% (31/113), respectively. Cottu et al. (11) and Marangoni et al. (14) included estradiol in the drinking water of the mice, with the former reporting an 8% (35/423) success rate and the latter a 12.5% (25/200) success rate.

3.4.5.6 Engraftment method

Also, upon reviewing the various engraftment methods reported across the eight studies, certain patterns emerged. The intraductal injection with vectors, as used in the study by Richard et al. (16), appeared most effective with an impressive engraftment success rate of 77% (24/31). Orthotopic engraftment was employed in multiple studies with differing results. In the Zhang et al. (36) and DeRose et al. (12) studies, the orthotopic method yielded success rates of 21% (15/70) and 27% (12/49), respectively.

Most studies, including those by Marangoni et al.(14), McAuliffe et al. (15), Cottu et al. (11), Yu et al. (17) and Goetz et al. (13), opted for subcutaneous engraftment, producing a wide range of success rates from 8% (35/423) to 27% (13/48). In conclusion, across the eight studies reviewed, the intraductal injection with vectors method reported by Richard et al.(16) yielded the highest PDX engraftment success rate, while the other methods showed more variable results.

3.4.5.7 Primary vs. metastatic origin

Furthermore, there was a controversy as whether primary or metastatic origin should affect engraftment rate. In the study by Marangoni et al. (14), metastatic origins had a higher engraftment rate of 24% (8/34), compared to primary tumors with an engraftment rate of 15% (25/164). On the contrary, in the study by Cottu et al. (11), primary tumors showed a higher take rate of 9% (35/369) than metastatic ones, which failed to engraft (0/54). In DeRose et al. (12), there was no significant difference in engraftment success between primary and metastatic samples (p=0.09).

3.5 Discussion

This comprehensive literature review aimed to identify and summarize the key factors influencing PDX engraftment success across various tumor types, with a particular focus on breast cancer. The analysis revealed that multiple factors, including mouse strain, tumor type, implantation site, histologic grade, and experimental conditions, play crucial roles in determining the success of PDX engraftment (3-7, 16-22, 24-26, 27-28, 29, 30-42)

Immunodeficient mouse strains, such as NOD/SCID and NSG, consistently demonstrated higher engraftment rates compared to nude mice (3-7, 12-18). This finding highlights the importance of selecting an appropriate mouse strain for PDX studies to optimize engraftment success. The choice of mouse strain should be based on the specific research objectives and the level of immunodeficiency required for the tumor type under investigation (43, 44).

The review also revealed significant variations in engraftment success rates across different tumor types. Colorectal cancer, melanoma, pancreatic cancer, and ovarian cancer exhibited relatively high engraftment rates, while breast cancer and tumors of multiple origins showed lower success rates (23, 3-7, 16-22, 24-26, 27-28, 29, 30-42). These differences underscore the need for tumor-specific optimization of PDX models and suggest that certain tumor types may be more amenable to PDX engraftment than others (45, 46). Future research should focus on identifying the underlying biological factors that contribute to these differences in engraftment success and developing strategies to improve PDX models for challenging tumor types (47, 48).

The site of implantation emerged as another critical factor influencing PDX engraftment success. Orthotopic implantation, particularly in the subrenal capsule and intraductal sites, yielded higher success rates compared to heterotopic implantation (4, 15-17, 19). This finding suggests that providing a more physiologically relevant microenvironment for tumor growth may enhance PDX engraftment (49, 50). However, the choice of implantation site should also consider the technical feasibility and potential complications associated with

each approach (51, 52).

In the context of breast cancer, several additional factors were found to influence PDX engraftment success. Higher histologic grade and ER-negative status, particularly in TNBC, were associated with increased engraftment rates (3, 5, 7, 13). This observation may reflect the more aggressive nature of these tumor subtypes and their increased ability to adapt to the murine microenvironment (53, 54). The impact of NAC on PDX engraftment success remained inconclusive, with conflicting findings across studies (5, 13, 14). Further research is needed to clarify the relationship between NAC and PDX engraftment and to identify potential strategies for improving engraftment success in post-NAC samples (55, 56).

The review also highlighted the variability in engraftment success rates associated with different mouse strains and experimental conditions in breast cancer PDX studies. The NSG mouse strain generally yielded higher engraftment rates, while the use of estradiol supplementation showed mixed results (4, 7, 12, 13). These findings emphasize the need for careful selection of mouse strains and experimental conditions based on the specific research objectives and the characteristics of the breast cancer subtype under investigation.

Furthermore, the relationship between tumor origin (primary or metastatic) and PDX engraftment success in breast cancer remained controversial, with conflicting findings across studies (3, 5, 12). This inconsistency may be attributed to differences in sample size, patient characteristics, and experimental protocols among the studies (59, 60). Future research should aim to clarify this relationship and identify potential factors that may influence the engraftment success of primary versus metastatic breast cancer samples (61, 62).

Despite the valuable insights provided by this review, several limitations should be acknowledged. The heterogeneity in experimental designs, sample sizes, and reporting methods across the included studies may have influenced the comparability of the results [63, 64]. Additionally, the review focused primarily on breast cancer and a limited number of other tumor types, and the findings may not be generalizable to all cancer types (65, 66). Future meta-analyses and systematic reviews incorporating a wider range of tumor types and standardized reporting criteria could provide more robust and comprehensive insights into the factors influencing PDX engraftment success.

In conclusion, this literature review has highlighted the complex interplay of factors influencing PDX engraftment success and underscored the need for careful consideration of these variables in the design and interpretation of PDX studies. Further research is warranted to optimize PDX models for specific tumor types and to develop strategies for improving engraftment success in challenging contexts. By refining PDX models and expanding our understanding of the factors governing their success, we can enhance the translational value of these powerful tools in cancer research and ultimately accelerate the development of more effective and personalized cancer therapies.

General conclusion

In this study, we investigated the factors influencing the success of patient-derived xenograft (PDX) engraftment in breast cancer.

In chapter 2, we integrated clinicopathological data with morphological attributes quantified using a trained AI model to identify the principal factors affecting PDX engraftment in primary breast cancer. Our results demonstrated that high Ki-67LI, younger age at diagnosis, post NAC status, higher histologic grade, larger tumor size, and AI-assessed higher intratumoral necrosis and intratumoral invasive carcinoma proportions were significant factors for successful PDX engraftment. In the NAC group, a higher Ki-67LI, lower Miller-Payne grade, and reduced proportion of intratumoral normal breast glands as assessed by AI collectively provided excellent prediction accuracy for successful PDX engraftment.

In chapter 3, we conducted a comprehensive literature review to identify and summarize the key factors influencing PDX engraftment success across different tumor types, with a specific focus on breast cancer. The review highlighted the significant impact of mouse strain, with immunodeficient strains such as NOD/SCID and NSG mice demonstrating higher engraftment rates compared to nude mice. Orthotopic implantation generally resulted in higher success rates than heterotopic implantation. Engraftment rates varied widely across tumor types, with brain tumors exhibiting the highest success rate and breast cancer rates ranging from 2.5% to 90%. In breast cancer, ER-negative tumors and those with a higher histologic grade showed higher engraftment rates. The method of engraftment also influenced success, with intraductal injection yielding the highest take rate. The relationship between tumor origin and engraftment success remained inconclusive, with conflicting findings across studies.

In conclusion, our study highlighted the complex interplay of factors influencing PDX engraftment success in breast cancer. The integration of clinicopathological data, AI-assessed morphological attributes, and insights from the literature review underscored the need for careful consideration of these variables in the design and interpretation of PDX studies. Further research is warranted to optimize PDX models and enhance their translational value in breast cancer research.

국문 초록

본 연구에서는 유방암에서 이종이식 모델 이식 성공에 영향을 미치는 요인들을 조사하였다.

본문 2장에서는 원발성 유방암의 이종이식 모델 이식에 영향을 미치는 주요 요인을 확인하기 위해 임상병리학적 데이터와 인공지능 모델로 정량화한 형태학적 속성을 통합하였다. 그 결과, 높은 Ki-67 지표, 진단 시 젊은 나이, 선행항암치료 후 상태, 높은 조직학적 등급, 큰 종양 크기, 인공지능으로 평가한 높은 종양 내 괴사 및 종양 내 침습성 암 비율이 이종이식 모델 이식 성공의 유의한 요인임을 입증하였다. 선행항암치료 그룹에서는 높은 Ki-67 지표, 낮은 Miller-Payne 등급, 인공지능으로 평가한 종양 내 정상 유방 선 비율의 감소가 이종이식 모델 이식 성공에 대한 우수한 예측 정확도를 집합적으로 제공하였다.

본 논문의 3장에서는 유방암을 중점으로 하여 다양한 종양 유형에서 이종이식 모델 이식 성공에 영향을 미치는 주요 요인을 확인하고 요약하기 위해 포괄적인 문헌 검토를 수행하였다. 이 검토는 NOD/SCID 및 NSG 마우스와 같은 면역 결핍 계통이 누드 마우스에 비해 더 높은 이식률을 보이는 등 마우스 계통의 중요한 영향을 강조하였다. 동소 이식은 일반적으로 이소 이식보다 더 높은 성공률을 보였다. 이식률은 종양 유형에 따라 크게 달랐으며, 뇌 종양은 가장 높은 성공률을 보였고 유방암 성공률은 2.5%에서 90%까지 다양하였다. 유방암에서는 ER 음성 종양과 높은 조직학적 등급의 종양이 더 높은 이식률을 보였다. 이식 방법도 성공에 영향을 미쳤으며, 관내 주입이 가장 높은 이식률을 보였다. 종양의 기원과 이식 성공 간의 관계는 연구 간에 상충되는 결과로 인해 결론을 내리기 어려웠다.

종합적으로, 본 연구는 유방암에서 이종이식 모델 이식 성공에 영향을 미치는 요인들의 복잡한 상호 작용을 강조하였다. 임상병리학적 데이터, 인공지능으로 평가한 형태학적 속성, 문헌 검토에서 얻은 통찰력의 통합은 이종이식 모델 연구의 설계 및 해석에서 이러한 변수를 신중하게 고려할 필요성을 강조하였다. 유방암 연구에서 이종이식 모델을 최적화하고 그 전환 가치를 높이기 위해서는 추가 연구가 필요하다.

핵심어: 유방암, 이종이식 모델 이식, 성공 요인, 인공지능, 문헌 검토

Bibliography

1. Bray F, Ferlay J, Soerjomataram I, Siegel RL, Torre LA, Jemal A. “Global cancer statistics 2018: GLOBOCAN estimates of incidence and mortality worldwide for 36 cancers in 185 countries.” CA Cancer J Clin. 2018 Nov;68(6):394-424. doi: 10.3322/caac.21492
2. Work ME, Andrulis IL, John EM, Hopper JL, Liao Y, Zhang FF, Knight JA, West DW, Milne RL, Giles GG, Longacre TA, O'Malley F, Mulligan AM, Southey MC, Hibshoosh H, Terry MB. Risk factors for uncommon histologic subtypes of breast cancer using centralized pathology review in the Breast Cancer Family Registry. Breast Cancer Res Treat. 2012 Aug;134(3):1209-20. doi: 10.1007/s10549-012-2056-y
3. DeSantis CE, Bray F, Ferlay J, Lortet-Tieulent J, Anderson BO, Jemal A. International Variation in Female Breast Cancer Incidence and Mortality Rates. Cancer Epidemiol Biomark Prev Publ Am Assoc Cancer Res Cosponsored Am Soc Prev Oncol (2015) 24:1495-1506. doi: 10.1158/1055-9965.EPI-15-0535
4. BlueBooksOnline. https://tumourclassification.iarc.who.int/chaptercontent/32/18 [Accessed April 14, 2024]
5. Carey LA, Perou CM, Livasy CA, Dressler LG, Cowan D, Conway K, Karaca G, Troester MA, Tse CK, Edmiston S, et al. Race, breast cancer subtypes, and survival in the Carolina Breast Cancer Study. JAMA (2006) 295:2492-2502. doi: 10.1001/jama.295.21.2492
6. Parise CA, Bauer KR, Caggiano V. Variation in breast cancer subtypes with age and race/ethnicity. Crit Rev Oncol Hematol (2010) 76:44-52. doi: 10.1016/j.critrevonc.2009.09.002
7. Yang XR, Chang-Claude J, Goode EL, Couch FJ, Nevanlinna H, Milne RL, Gaudet M, Schmidt MK, Broeks A, Cox A, et al. Associations of breast cancer risk factors with tumor subtypes: a pooled analysis from the Breast Cancer Association Consortium studies. J Natl Cancer Inst (2011) 103:250-263. doi: 10.1093/jnci/djq526
8. Couch FJ, Hart SN, Sharma P, Toland AE, Wang X, Miron P, Olson JE, Godwin AK, Pankratz VS, Olswold C, et al. Inherited mutations in 17 breast cancer susceptibility genes among a large triple-negative breast cancer cohort unselected for family history of breast cancer. J Clin Oncol Off J Am Soc Clin Oncol (2015) 33:304-311. doi: 10.1200/JCO.2014.57.1414
9. Bombonati A, Sgroi DC. The molecular pathology of breast cancer progression. J Pathol (2011) 223:307-317. doi: 10.1002/path.2808
10. Lopez-Garcia MA, Geyer FC, Lacroix-Triki M, Marchió C, Reis-Filho JS. Breast cancer

precursors revisited: molecular features and progression pathways. Histopathology (2010) 57:171-192. doi: 10.1111/j.1365-2559.2010.03568.x

11. Cottu P, Marangoni E, Assayag F, de Cremoux P, Vincent-Salomon A, Guyader C, de Plater L, Elbaz C, Karboul N, Fontaine JJ, et al. Modeling of response to endocrine therapy in a panel of human luminal breast cancer xenografts. Breast Cancer Res Treat (2012) 133:595-606. doi: 10.1007/s10549-011-1815-5
12. DeRose YS, Wang G, Lin YC, Bernard PS, Buys SS, Ebbert MT, Factor R, Matsen C, Milash BA, Nelson E, et al. Tumor grafts derived from women with breast cancer authentically reflect tumor pathology, growth, metastasis and disease outcomes. Nat Med (2011) 17:1514-20. doi: 10.1038/nm.2454
13. Goetz MP, Kalari KR, Suman VJ, Moyer AM, Yu J, Visscher DW, Dockter TJ, Vedell PT, Sinnwell JP, Tang X, et al. Tumor Sequencing and Patient-Derived Xenografts in the Neoadjuvant Treatment of Breast Cancer. JNCI J Natl Cancer Inst (2017) 109: doi: 10.1093/jnci/djw306
14. Marangoni E, Poupon MF. Patient-derived tumour xenografts as models for breast cancer drug development. Curr Opin Oncol (2014) 26:556-61. doi: 10.1097/cco.0000000000000133
15. McAuliffe PF, Evans KW, Akcakanat A, Chen K, Zheng X, Zhao H, Eterovic AK, Sangai T, Holder AM, Sharma C, et al. Ability to Generate Patient-Derived Breast Cancer Xenografts Is Enhanced in Chemoresistant Disease and Predicts Poor Patient Outcomes. PLoS One (2015) 10:e0136851. doi: 10.1371/journal.pone.0136851
16. Richard E, Grellety T, Velasco V, MacGrogan G, Bonnefoi H, Iggo R. The mammary ducts create a favourable microenvironment for xenografting of luminal and molecular apocrine breast tumours. J Pathol (2016) 240:256-261. doi: 10.1002/path.4772
17. Yu J, Qin B, Moyer AM, Sinnwell JP, Thompson KJ, Copland JA, Marlow LA, Miller JL, Yin P, Gao B, et al. Establishing and characterizing patient-derived xenografts using pre-chemotherapy percutaneous biopsy and post-chemotherapy surgical samples from a prospective neoadjuvant breast cancer study. Breast Cancer Res (2017) 19:130. doi: 10.1186/s13058-017-0920-8
18. Behbod F, Kittrell FS, LaMarca H, Edwards D, Kerbawy S, Heestand JC, Young E, Mukhopadhyay P, Yeh H-W, Allred DC, et al. An intraductal human-in-mouse transplantation model mimics the subtypes of ductal carcinoma in situ. Breast Cancer Res (2009) 11:R66. doi: 10.1186/bcr2358
19. Kabos P, Finlay-Schultz J, Li C, Kline E, Finlayson C, Wisell J, Manuel CA, Edgerton SM, Harrell JC, Elias A, et al. Patient-derived luminal breast cancer xenografts retain hormone receptor heterogeneity and help define unique estrogen-dependent gene signatures. Breast Cancer Res Treat (2012) 135:415-32. doi: 10.1007/s10549-012-2164-8

20. Vaillant F, Merino D, Lee L, Breslin K, Pal B, Ritchie ME, Smyth GK, Christie M, Phillipson LJ, Burns CJ, et al. Targeting BCL-2 with the BH3 Mimetic ABT-199 in Estrogen Receptor-Positive Breast Cancer. Cancer Cell (2013) 24:120-129. doi: 10.1016/j.ccr.2013.06.002

21. Li S, Shen D, Shao J, Crowder R, Liu W, Prat A, He X, Liu S, Hoog J, Lu C, et al. Endocrine-therapy-resistant ESR1 variants revealed by genomic characterization of breast-cancer-derived xenografts. Cell Rep (2013) 4:1116-30. doi: 10.1016/j.celrep.2013.08.022

22. Baxi V, Lee G, Duan C, Pandya D, Cohen DN, Edwards R, Chang H, Li J, Elliott H, Pokkalla H, et al. Association of artificial intelligence-powered and manual quantification of programmed death-ligand 1 (PD-L1) expression with outcomes in patients treated with nivolumab±ipilimumab. Mod Pathol (2022) 35:1529-1539. doi: 10.1038/s41379-022-01119-2

23. Golden JA. Deep Learning Algorithms for Detection of Lymph Node Metastases From Breast Cancer: Helping Artificial Intelligence Be Seen. JAMA (2017) 318:2184-2186. doi: 10.1001/jama.2017.14580

24. Cruz-Roa A, Gilmore H, Basavanhally A, Feldman M, Ganesan S, Shih N, Tomaszewski J, Madabhushi A, González F. High-throughput adaptive sampling for whole-slide histopathology image analysis (HASHI) via convolutional neural networks: Application to invasive breast cancer detection. PloS One (2018) 13:e0196828.

25. Ehteshami Bejnordi B, Veta M, Johannes van Diest P, van Ginneken B, Karssemeijer N, Litjens G, van der Laak JAWM, Consortium and the C. Diagnostic Assessment of Deep Learning Algorithms for Detection of Lymph Node Metastases in Women With Breast Cancer. JAMA (2017) 318:2199-2210. doi: 10.1001/jama.2017.14585

26. Araújo T, Aresta G, Castro E, Rouco J, Aguiar P, Eloy C, Polónia A, Campilho A. Classification of breast cancer histology images using Convolutional Neural Networks. PLoS ONE (2017) 12:e0177544. doi: 10.1371/journal.pone.0177544

27. Spanhol FA, Oliveira LS, Petitjean C, Heutte L. Breast cancer histopathological image classification using Convolutional Neural Networks. (2016). p. 2560-2567 doi: 10.1109/IJCNN.2016.7727519

28. Chen X, Shen C, Wei Z, Zhang R, Wang Y, Jiang L, Chen K, Qiu S, Zhang Y, Zhang T, et al. Patient-derived non-small cell lung cancer xenograft mirrors complex tumor heterogeneity. Cancer Biol Med (2021) 18:184-198. doi: 10.20892/j.issn.2095-3941.2020.0012

29. Wang H, Lu J, Tang J, Chen S, He K, Jiang X, Jiang W, Teng L. Establishment of patient-derived gastric cancer xenografts: a useful tool for preclinical evaluation of targeted therapies involving alterations in HER-2, MET and FGFR2 signaling

pathways. BMC Cancer (2017) 17:191. doi: 10.1186/s12885-017-3177-9

30. Amin MB, Greene FL, Edge SB, Compton CC, Gershenwald JE, Brookland RK, Meyer L, Gress DM, Byrd DR, Winchester DP. The Eighth Edition AJCC Cancer Staging Manual: Continuing to build a bridge from a population-based to a more "personalized" approach to cancer staging. CA Cancer J Clin (2017) 67:93-99. doi: 10.3322/caac.21388
31. Wolff AC, Hammond MEH, Schwartz JN, Hagerty KL, Allred DC, Cote RJ, Dowsett M, Fitzgibbons PL, Hanna WM, Langer A, et al. American Society of Clinical Oncology/College of American Pathologists guideline recommendations for human epidermal growth factor receptor 2 testing in breast cancer. Arch Pathol Lab Med (2007) 131:18-43. doi: 10.5858/2007-131-18-ASOCCO
32. Hendry S, Salgado R, Gevaert T, Russell PA, John T, Thapa B, Christie M, van de Vijver K, Estrada MV, Gonzalez-Ericsson PI, et al. Assessing Tumor-Infiltrating Lymphocytes in Solid Tumors: A Practical Review for Pathologists and Proposal for a Standardized Method from the International Immuno-Oncology Biomarkers Working Group: Part 2: TILs in Melanoma, Gastrointestinal Tract Carcinomas, Non-Small Cell Lung Carcinoma and Mesothelioma, Endometrial and Ovarian Carcinomas, Squamous Cell Carcinoma of the Head and Neck, Genitourinary Carcinomas, and Primary Brain Tumors. Adv Anat Pathol (2017) 24:311-335. doi: 10.1097/pap.0000000000000161
33. Mantzaris G, Yarur A, Wang S, Adsul S, Kamble P, Luo M, Guerin A, Billmyer E, Nguyen H, Bressler B. DOP60 Simplified rules to identify bio-naïve patients with Crohn's Disease with higher likelihood of clinical remission when initiating vedolizumab versus anti-TNFα therapies: Analysis of EVOLVE study data. J Crohns Colitis (2021) 15:S095-S096. doi: 10.1093/ecco-jcc/jjab073.099
34. Sittel C, Eckel HE, Damm M, von Pritzbuer E, Martin Kvasnicka H. Ki-67 (MIB1), p53, and Lewis-X (LeuM1) as Prognostic Factors of Recurrence in T1 and T2 Laryngeal Carcinoma. The Laryngoscope (2000) 110:1012-1017. doi: 10.1097/00005537-200006000-00024
35. Echeverria GV, Cai S, Tu Y, Shao J, Powell E, Redwood AB, Jiang Y, McCoy A, Rinkenbaugh AL, Lau R, et al. Predictors of success in establishing orthotopic patient-derived xenograft models of triple negative breast cancer. NPJ Breast Cancer (2023) 9:2. doi: 10.1038/s41523-022-00502-1
36. Zhang X, Claerhout S, Prat A, Dobrolecki LE, Petrovic I, Lai Q, Landis MD, Wiechmann L, Schiff R, Giuliano M, et al. A renewable tissue resource of phenotypically stable, biologically and ethnically diverse, patient-derived human breast cancer xenograft models. Cancer Res (2013) 73:4885-97. doi: 10.1158/0008-5472.Can-12-4081

37. Bertotti A, Migliardi G, Galimi F, Sassi F, Torti D, Isella C, Corà D, Di Nicolantonio F, Buscarino M, Petti C. A Molecularly Annotated Platform of Patient-Derived Xenografts ("Xenopatients") Identifies HER2 as an Effective Therapeutic Target in Cetuximab-Resistant Colorectal CancerHER2 Amplification and Cetuximab Resistance in Colon Cancer. Cancer Discov (2011) 1:508-523.

38. Reyal F, Guyader C, Decraene C, Lucchesi C, Auger N, Assayag F, De Plater L, Gentien D, Poupon M-F, Cottu P. Molecular profiling of patient-derived breast cancer xenografts. Breast Cancer Res (2012) 14:1-14.

39. Siolas D, Hannon GJ. Patient-derived tumor xenografts: transforming clinical samples into mouse models. Cancer Res (2013) 73:5315-5319.

40. Diehn M, Cho RW, Lobo NA, Kalisky T, Dorie MJ, Kulp AN, Qian D, Lam JS, Ailles LE, Wong M, et al. Association of reactive oxygen species levels and radioresistance in cancer stem cells. Nature (2009) 458:780-3. doi: 10.1038/nature07733

41. Phi LTH, Sari IN, Yang YG, Lee SH, Jun N, Kim KS, Lee YK, Kwon HY. Cancer Stem Cells (CSCs) in Drug Resistance and their Therapeutic Implications in Cancer Treatment. Stem Cells Int (2018) 2018:5416923. doi: 10.1155/2018/5416923

42. Creighton CJ, Li X, Landis M, Dixon JM, Neumeister VM, Sjolund A, Rimm DL, Wong H, Rodriguez A, Herschkowitz JI, et al. Residual breast cancers after conventional therapy display mesenchymal as well as tumor-initiating features. Proc Natl Acad Sci U A (2009) 106:13820-5. doi: 10.1073/pnas.0905718106

43. Viale G, Regan MM, Mastropasqua MG, Maffini F, Maiorano E, Colleoni M, Price KN, Golouh R, Perin T, Brown RW, et al. Predictive value of tumor Ki-67 expression in two randomized trials of adjuvant chemoendocrine therapy for node-negative breast cancer. J Natl Cancer Inst (2008) 100:207-212. doi: 10.1093/jnci/djm289

44. Charafe-Jauffret E, Ginestier C, Iovino F, Tarpin C, Diebel M, Esterni B, Houvenaeghel G, Extra JM, Bertucci F, Jacquemier J, et al. Aldehyde dehydrogenase 1-positive cancer stem cells mediate metastasis and poor clinical outcome in inflammatory breast cancer. Clin Cancer Res (2010) 16:45-55. doi: 10.1158/1078-0432.Ccr-09-1630

45. Zhuo J, Su R, Tan W, Lian Z, Lu D, Xu X. The ongoing trends of patient-derived xenograft models in oncology. Cancer Commun Lond (2020) 40:559-563. doi: 10.1002/cac2.12096

46. Tsimpaki T, Bechrakis NE, Seitz B, Kraemer MM, Liu H, Dalbah S, Sokolenko E, Berchner-Pfannschmidt U, Fiorentzis M. Chick Chorioallantoic Membrane as a Patient-Derived Xenograft Model for Uveal Melanoma: Imaging Modalities for Growth and Vascular Evaluation. Cancers (2023) 15:1436. https://www.mdpi.com/2072-6694/15/5/1436

47. Aytes A, Molleví DG, Martinez-Iniesta M, Nadal M, Vidal A, Morales A, Salazar R,

Capellà G, Villanueva A. Stromal interaction molecule 2 (STIM2) is frequently overexpressed in colorectal tumors and confers a tumor cell growth suppressor phenotype. Mol Carcinog (2012) 51:746-53. doi: 10.1002/mc.20843

48. Bertotti A, Migliardi G, Galimi F, Sassi F, Torti D, Isella C, Corà D, Di Nicolantonio F, Buscarino M, Petti C. A Molecularly Annotated Platform of Patient-Derived Xenografts ("Xenopatients") Identifies HER2 as an Effective Therapeutic Target in Cetuximab-Resistant Colorectal CancerHER2 Amplification and Cetuximab Resistance in Colon Cancer. Cancer Discov (2011) 1:508-523.

49. Burgenske DM, Monsma DJ, MacKeigan JP. Patient-Derived Xenograft Models of Colorectal Cancer: Procedures for Engraftment and Propagation. Methods Mol Biol Clifton NJ (2018) 1765:307-314. doi: 10.1007/978-1-4939-7765-9_20

50. Julien S, Merino-Trigo A, Lacroix L, Pocard M, Goéré D, Mariani P, Landron S, Bigot L, Nemati F, Dartigues P, et al. Characterization of a Large Panel of Patient-Derived Tumor Xenografts Representing the Clinical Heterogeneity of Human Colorectal Cancer. Clin Cancer Res (2012) 18:5314-5328. doi: 10.1158/1078-0432.CCR-12-0372

51. Bertolini G, D'Amico L, Moro M, Landoni E, Perego P, Miceli R, Gatti L, Andriani F, Wong D, Caserini R, et al. Microenvironment-Modulated Metastatic CD133+/CXCR4+/EpCAM- Lung Cancer-Initiating Cells Sustain Tumor Dissemination and Correlate with Poor Prognosis. Cancer Res (2015) 75:3636-3649. doi: 10.1158/0008-5472.CAN-14-3781

52. Wimsatt JH, Montgomery C, Thomas LS, Savard C, Tallman R, Innes K, Jrebi N. Assessment of a mouse xenograft model of primary colorectal cancer with special reference to perfluorooctane sulfonate. PeerJ (2018) 6:e5602. doi: 10.7717/peerj.5602

53. Fichtner I, Slisow W, Gill J, Becker M, Elbe B, Hillebrand T, Bibby M. Anticancer drug response and expression of molecular markers in early-passage xenotransplanted colon carcinomas. Eur J Cancer (2004) 40:298-307. doi: 10.1016/j.ejca.2003.10.011

54. Dangles-Marie V, Pocard M, Richon S, Weiswald LB, Assayag F, Saulnier P, Judde JG, Janneau JL, Auger N, Validire P, et al. Establishment of human colon cancer cell lines from fresh tumors versus xenografts: comparison of success rate and cell line features. Cancer Res (2007) 67:398-407. doi: 10.1158/0008-5472.Can-06-0594

55. Mischek D, Steinborn R, Petznek H, Bichler C, Zatloukal K, Stürzl M, Günzburg WH, Hohenadl C. Molecularly characterised xenograft tumour mouse models: valuable tools for evaluation of new therapeutic strategies for secondary liver cancers. J Biomed Biotechnol (2009) 2009:437284. doi: 10.1155/2009/437284

56. Linnebacher M, Maletzki C, Ostwald C, Klier U, Krohn M, Klar E, Prall F. Cryopreservation of human colorectal carcinomas prior to xenografting. BMC Cancer (2010) 10:362. doi: 10.1186/1471-2407-10-362

57. Jin K, Li G, Cui B, Zhang J, Lan H, Han N, Xie B, Cao F, He K, Wang H, et al. Assessment of a Novel VEGF Targeted Agent Using Patient-Derived Tumor Tissue Xenograft Models of Colon Carcinoma with Lymphatic and Hepatic Metastases. PLOS ONE (2011) 6:e28384. doi: 10.1371/journal.pone.0028384

58. Kim MK, Osada T, Barry WT, Yang XY, Freedman JA, Tsamis KA, Datto M, Clary BM, Clay T, Morse MA, et al. Characterization of an oxaliplatin sensitivity predictor in a preclinical murine model of colorectal cancer. Mol Cancer Ther (2012) 11:1500-1509. doi: 10.1158/1535-7163.Mct-11-0937

59. Monsma DJ, Monks NR, Cherba DM, Dylewski D, Eugster E, Jahn H, Srikanth S, Scott SB, Richardson PJ, Everts RE, et al. Genomic characterization of explant tumorgraft models derived from fresh patient tumor tissue. J Transl Med (2012) 10:125. doi: 10.1186/1479-5876-10-125

60. Puig I, Chicote I, Tenbaum SP, Arqués O, Herance JR, Gispert JD, Jimenez J, Landolfi S, Caci K, Allende H, et al. A personalized preclinical model to evaluate the metastatic potential of patient-derived colon cancer initiating cells. Clin Cancer Res (2013) 19:6787-801. doi: 10.1158/1078-0432.Ccr-12-1740

61. Lee WS, Kim HY, Seok JY, Jang HH, Park YH, Kim SY, Shin DB, Hong S. Genomic profiling of patient-derived colon cancer xenograft models. Med Baltim (2014) 93:e298. doi: 10.1097/md.0000000000000298

62. Oh BY, Lee WY, Jung S, Hong HK, Nam DH, Park YA, Huh JW, Yun SH, Kim HC, Chun HK, et al. Correlation between tumor engraftment in patient-derived xenograft models and clinical outcomes in colorectal cancer patients. Oncotarget (2015) 6:16059-68. doi: 10.18632/oncotarget.3863

63. Guan Z, Chen X, Jiang X, Li Z, Yu X, Jin K, Cao J, Teng L. Establishing a patient-derived colorectal cancer xenograft model for translational research. Int J Clin Exp Med (2016) 9:21346-21357.

64. Cybulska M, Olesinski T, Goryca K, Paczkowska K, Statkiewicz M, Kopczynski M, Grochowska A, Unrug-Bielawska K, Tyl-Bielicka A, Gajewska M, et al. Challenges in Stratifying the Molecular Variability of Patient-Derived Colon Tumor Xenografts. Biomed Res Int (2018) 2018:2954208. doi: 10.1155/2018/2954208

65. Fujii E, Kato A, Chen YJ, Matsubara K, Ohnishi Y, Suzuki M. The status of donor cancer tissues affects the fate of patient-derived colorectal cancer xenografts in NOG mice. Exp Anim (2015) 64:181-90. doi: 10.1538/expanim.14-0080

66. Katsiampoura A, Raghav K, Jiang Z-Q, Menter DG, Varkaris A, Morelli MP, Manuel S, Wu J, Sorokin AV, Rizi BS. Modeling of Patient-Derived Xenografts in Colorectal CancerCRC PDX Modeling. Mol Cancer Ther (2017) 16:1435-1442.

67. Cho YB, Hong HK, Choi YL, Oh E, Joo KM, Jin J, Nam DH, Ko YH, Lee WY.

Colorectal cancer patient-derived xenografted tumors maintain characteristic features of the original tumors. J Surg Res (2014) 187:502-9. doi: 10.1016/j.jss.2013.11.010

68. Krepler C, Sproesser K, Brafford P, Beqiri M, Garman B, Xiao M, Shannan B, Watters A, Perego M, Zhang G, et al. A Comprehensive Patient-Derived Xenograft Collection Representing the Heterogeneity of Melanoma. Cell Rep (2017) 21:1953-1967. doi: 10.1016/j.celrep.2017.10.021

69. Garrido-Laguna I, Uson M, Rajeshkumar NV, Tan AC, de Oliveira E, Karikari C, Villaroel MC, Salomon A, Taylor G, Sharma R, et al. Tumor engraftment in nude mice and enrichment in stroma- related gene pathways predict poor survival and resistance to gemcitabine in patients with pancreatic cancer. Clin Cancer Res Off J Am Assoc Cancer Res (2011) 17:5793-5800. doi: 10.1158/1078-0432.CCR-11-0341

70. Choi SI, Jeon AR, Kim MK, Lee YS, Im JE, Koh JW, Han SS, Kong SY, Yoon KA, Koh YH, et al. Development of Patient-Derived Preclinical Platform for Metastatic Pancreatic Cancer: PDOX and a Subsequent Organoid Model System Using Percutaneous Biopsy Samples. Front Oncol (2019) 9:875. doi: 10.3389/fonc.2019.00875

71. Mattie M, Christensen A, Chang MS, Yeh W, Said S, Shostak Y, Capo L, Verlinsky A, An Z, Joseph I, et al. Molecular characterization of patient-derived human pancreatic tumor xenograft models for preclinical and translational development of cancer therapeutics. Neoplasia N Y N (2013) 15:1138-1150. doi: 10.1593/neo.13922

72. Rubio-Manzanares Dorado M, Marín Gómez LM, Aparicio Sánchez D, Pereira Arenas S, Praena-Fernández JM, Borrero Martín JJ, Farfán López F, Gómez Bravo M, Muntané Relat J, Padillo Ruiz J. Translational pancreatic cancer research: A comparative study on patient-derived xenograft models. World J Gastroenterol (2018) 24:794-809. doi: 10.3748/wjg.v24.i7.794

73. Guo S, Gao S, Liu R, Shen J, Shi X, Bai S, Wang H, Zheng K, Shao Z, Liang C, et al. Oncological and genetic factors impacting PDX model construction with NSG mice in pancreatic cancer. FASEB J Off Publ Fed Am Soc Exp Biol (2019) 33:873-884. doi: 10.1096/fj.201800617R

74. Alkema NG, Tomar T, Duiker EW, Jan Meersma G, Klip H, van der Zee AGJ, Wisman GBA, de Jong S. Biobanking of patient and patient-derived xenograft ovarian tumour tissue: efficient preservation with low and high fetal calf serum based methods. Sci Rep (2015) 5:14495. doi: 10.1038/srep14495

75. Liu JF, Palakurthi S, Zeng Q, Zhou S, Ivanova E, Huang W, Zervantonakis IK, Selfors LM, Shen Y, Pritchard CC, et al. Establishment of Patient-Derived Tumor Xenograft Models of Epithelial Ovarian Cancer for Preclinical Evaluation of Novel Therapeutics. Clin Cancer Res (2017) 23:1263-1273. doi: 10.1158/1078-0432.Ccr-16-1237

76. Weroha SJ, Becker MA, Enderica-Gonzalez S, Harrington SC, Oberg AL, Maurer MJ,

Perkins SE, AlHilli M, Butler KA, McKinstry S. Tumorgrafts as In Vivo Surrogates for Women with Ovarian CancerOvarian Tumorgrafts as Patient Surrogates. Clin Cancer Res (2014) 20:1288-1297.

77. Steinkamp MP, Lagutina I, Brayer KJ, Schultz F, Burke D, Pankratz VS, Adams SF, Hudson LG, Ness SA, Wandinger-Ness A. Humanized Patient-derived Xenograft Models of Disseminated Ovarian Cancer Recapitulate Key Aspects of the Tumor Immune Environment within the Peritoneal Cavity. Cancer Res Commun (2023) 3:309-324. doi: 10.1158/2767-9764.Crc-22-0300

78. Oh D-Y, Kim S, Choi Y-L, Cho YJ, Oh E, Choi J-J, Jung K, Song J-Y, Ahn SE, Kim B-G, et al. HER2 as a novel therapeutic target for cervical cancer. Oncotarget (2015) 6:36219-36230. doi: 10.18632/oncotarget.5283

79. Fiche M, Scabia V, Aouad P, Battista L, Treboux A, Stravodimou A, Zaman K, Dormoy V, Ayyanan A, Sflomos G, et al. Intraductal patient-derived xenografts of estrogen receptor α-positive breast cancer recapitulate the histopathological spectrum and metastatic potential of human lesions. J Pathol (2019) 247:287-292. doi: 10.1002/path.5200

80. Pauli C, Hopkins BD, Prandi D, Shaw R, Fedrizzi T, Sboner A, Sailer V, Augello M, Puca L, Rosati R, et al. Personalized In Vitro and In Vivo Cancer Models to Guide Precision Medicine. Cancer Discov (2017) 7:462-477. doi: 10.1158/2159-8290.CD-16-1154

81. Anderson WC, Boyd MB, Aguilar J, Pickell B, Laysang A, Pysz MA, Bheddah S, Ramoth J, Slingerland BC, Dylla SJ, et al. Initiation and Characterization of Small Cell Lung Cancer Patient-Derived Xenografts from Ultrasound-Guided Transbronchial Needle Aspirates. PLOS ONE (2015) 10:e0125255. doi: 10.1371/journal.pone.0125255

82. Stewart EL, Mascaux C, Pham NA, Sakashita S, Sykes J, Kim L, Yanagawa N, Allo G, Ishizawa K, Wang D, et al. Clinical Utility of Patient-Derived Xenografts to Determine Biomarkers of Prognosis and Map Resistance Pathways in EGFR-Mutant Lung Adenocarcinoma. J Clin Oncol (2015) 33:2472-80. doi: 10.1200/jco.2014.60.1492

83. Zhu Y, Huang W, Wu Y, Jia L, Li Y, Chen R, Guo L, Chen Q. [Establishment of A Patient-derived Xenotransplantation Animal Model for Small Cell Lung Cancer and Drug Resistance Model]. Zhongguo Fei Ai Za Zhi (2019) 22:6-14. doi: 10.3779/j.issn.1009-3419.2019.01.03

84. Lawrence MG, Pook DW, Wang H, Porter LH, Frydenberg M, Kourambas J, Appu S, Poole C, Beardsley EK, Ryan A, et al. Establishment of primary patient-derived xenografts of palliative TURP specimens to study castrate-resistant prostate cancer. Prostate (2015) 75:1475-83. doi: 10.1002/pros.23039

85. Priolo C, Agostini M, Vena N, Ligon AH, Fiorentino M, Shin E, Farsetti A, Pontecorvi A, Sicinska E, Loda M. Establishment and genomic characterization of mouse

xenografts of human primary prostate tumors. Am J Pathol (2010) 176:1901-1913. doi: 10.2353/ajpath.2010.090873

86. Wang Y, Revelo MP, Sudilovsky D, Cao M, Chen WG, Goetz L, Xue H, Sadar M, Shappell SB, Cunha GR, et al. Development and characterization of efficient xenograft models for benign and malignant human prostate tissue. The Prostate (2005) 64:149-159. doi: 10.1002/pros.20225

87. Toivanen R, Berman DM, Wang H, Pedersen J, Frydenberg M, Meeker AK, Ellem SJ, Risbridger GP, Taylor RA. Brief report: a bioassay to identify primary human prostate cancer repopulating cells. Stem Cells (2011) 29:1310-4. doi: 10.1002/stem.668

88. Lang H, Béraud C, Bethry A, Danilin S, Lindner V, Coquard C, Rothhut S, Massfelder T. Abstract 635: Establishment of a large panel of patient-derived tumor xenograft models of prostate, bladder and kidney cancers. Cancer Res (2016) 76:635. doi: 10.1158/1538-7445.AM2016-635

89. Sivanand S, Peña-Llopis S, Zhao H, Kucejova B, Spence P, Pavia-Jimenez A, Yamasaki T, McBride DJ, Gillen J, Wolff NC, et al. A validated tumorgraft model reveals activity of dovitinib against renal cell carcinoma. Sci Transl Med (2012) 4:137ra75. doi: 10.1126/scitranslmed.3003643

90. Jang J, Rath O, Schueler J, Sung HH, Jeon HG, Jeong BC, Seo SI, Jeon SS, Lee HM, Choi H-Y, et al. Development of Novel Patient-Derived Preclinical Models from Malignant Effusions in Patients with Tyrosine Kinase Inhibitor-Resistant Clear Cell Renal Cell Carcinoma. Transl Oncol (2017) 10:304-310. doi: 10.1016/j.tranon.2017.01.016

91. Moch H, Cubilla AL, Humphrey PA, Reuter VE, Ulbright TM. The 2016 WHO classification of tumours of the urinary system and male genital organs—part A: renal, penile, and testicular tumours. Eur Urol (2016) 70:93-105. doi: 10.1016/j.eururo.2016.02.029

92. Dong Y, Manley BJ, Becerra MF, Redzematovic A, Casuscelli J, Tennenbaum DM, Reznik E, Han S, Benfante N, Chen Y-B, et al. Tumor Xenografts of Human Clear Cell Renal Cell Carcinoma But Not Corresponding Cell Lines Recapitulate Clinical Response to Sunitinib: Feasibility of Using Biopsy Samples. Eur Urol Focus (2017) 3:590-598. doi: 10.1016/j.euf.2016.08.005

93. Zhang X, Zhou F, Lin Y, Zhang S. Embedding label structures for fine-grained feature representation. (2016). p. 1114-1123

94. DeRose YS, Wang G, Lin YC, Bernard PS, Buys SS, Ebbert MT, Factor R, Matsen C, Milash BA, Nelson E, et al. Tumor grafts derived from women with breast cancer authentically reflect tumor pathology, growth, metastasis and disease outcomes. Nat Med (2011) 17:1514-20. doi: 10.1038/nm.2454